Superfluid effects on thermal evolution and rotational dynamics of neutron stars
by Michelle Beauvais Larson

A dissertation submitted in partial fulfillment of the requirements for the degree of Doctor of Philosophy in Physics
Montana State University

Abstract:
This thesis examines the observational consequences of superfluidity on thermal evolution and rotational dynamics of neutron stars. Temperature measurements of older neutron stars (tage >~ 10^6 yrs) indicate that these objects are heated. A promising candidate heat source is friction due to differential rotation between the neutron star crust and the superfluid it is thought to contain. We study the effects of superfluid friction on the long-term thermal and rotational evolution of a neutron star and obtain constraints on the strength of the frictional coupling between the stellar crust and the interior superfluid. The second part of this thesis provides simulations of glitches (sudden jumps in spin rate) in isolated pulsars. With the aim of distinguishing among different theoretical explanations for the glitch phenomenon, we study the response of a neutron star to two types of perturbations to the vortex array that threads the superfluid interior. Both mechanisms produce acceptable fits to glitch observations in the four pulsars we study. The two models make different predictions for the generation of internal heat and subsequent enhancement of surface emission. Future glitch observations coordinated with surface emission measurements will play a key role in distinguishing between the two glitch models we investigate.

SUPERFLUID EFFECTS ON THERMAL EVOLUTION AND ROTATIONAL DYNAMICS OF NEUTRON STARS

by

Michelle Beauvais Larson

A dissertation submitted in partial fulfillment
of the requirements for the degree

of

Doctor of Philosophy

in

Physics

MONTANA STATE UNIVERSITY
Bozeman, Montana

April 2001

APPROVAL

of a dissertation submitted by

Michelle Beauvais Larson

This dissertation has been read by each member of the dissertation committee and has been found to be satisfactory regarding content, English usage, format, citations, bibliographic style, and consistency, and is ready for submission to the College of Graduate Studies.

Bennett Link Bennett Link (Signature) 4/2/01 Date

Approved for the Department of Physics

John C. Hermanson (Signature) 4-2-01 Date

Approved for the College of Graduate Studies

Bruce R. McLeod Bruce R. McLeod (Signature) 4-5-01 Date

STATEMENT OF PERMISSION TO USE

In presenting this dissertation in partial fulfillment of the requirements for a doctoral degree at Montana State University, I agree that the Library shall make it available to borrowers under rules of the Library. I further agree that copying of this dissertation is allowable only for scholarly purposes, consistent with "fair use" as prescribed in the U. S. Copyright Law. Requests for extensive copying or reproduction of this dissertation should be referred to Bell & Howell Information and Learning, 300 North Zeeb Road, Ann Arbor, Michigan 48106, to whom I have granted "the exclusive right to reproduce and distribute my dissertation in and from microform along with the non-exclusive right to reproduce and distribute my abstract in any format in whole or in part."

Signature Michelle Beaudris Larson

Date 04/02/01

The Road Not Taken

Two roads diverged in a yellow wood,
And sorry I could not travel both
And be one traveler, long I stood
And looked down one as far as I could
To where it bent in the undergrowth;

Then took the other, as just as fair,
And having perhaps the better claim,
Because it was grassy and wanted wear;
Though as for that the passing there
Had worn them really about the same,

And both that morning equally lay
In leaves no step had troden black.
Oh, I kept the first for another day!
Yet knowing how way leads on to way,
I doubted if I should ever come back.

I shall be telling this with a sigh
Somewhere ages and ages hence:
Two roads diverged in a wood, and I-
I took the one less traveled by,
And that has made all the difference.

- Robert Frost

ACKNOWLEDGMENTS

I thank my advisor, Dr. Bennett Link, for his guidance in this research endeavor. I am grateful for all he has done to help develop the research scientist within me. I acknowledge the Montana Space Grant Consortium for financial support, and I thank its director, Dr. William Hiscock, for believing in me and my reasons for choosing this career path. I am deeply appreciative of the MSU solar physics group for adopting me into their professional family. My experience with the Yohkoh Public Outreach Project was pivotal in helping me find direction in my professional life. Overall, my association with the solar physics community has been paramount in making my graduate experience an intellectually stimulating and enjoyable one.

I am grateful to my father, Tom Beauvais, for always insisting that I support my opinions with sound, logical reasoning; he has helped me become better a scientist. I thank my mother, Peggy Beauvais, for encouraging me to follow my dreams, and for her interest and support in the ones I've chosen to pursue. I thank Pat Larson for introducing me to the world of sundials, which led to the creation of my most popular outreach activity, and Larry Larson for his valuable advice on how to successfully traverse the rocky road of graduate school.

Finally, I wholeheartedly thank my husband, Shane Larson, without whose support I would not have finished this degree. Shane's enthusiasm for research is highly contagious, and he pulled me through the times when my own was lacking. Shane never let me lose sight of my goals, and I am indebted to no one more than him for this achievement.

TABLE OF CONTENTS

LIST OF TABLES

LIST OF FIGURES

ABSTRACT

This thesis examines the observational consequences of superfluidity on thermal evolution and rotational dynamics of neutron stars. Temperature measurements of older neutron stars ($t_{\rm age} \gtrsim 10^6$ yrs) indicate that these objects are heated. A promising candidate heat source is friction due to differential rotation between the neutron star crust and the superfluid it is thought to contain. We study the effects of superfluid friction on the long-term thermal and rotational evolution of a neutron star and obtain constraints on the strength of the frictional coupling between the stellar crust and the interior superfluid. The second part of this thesis provides simulations of glitches (sudden jumps in spin rate) in isolated pulsars. With the aim of distinguishing among different theoretical explanations for the glitch phenomenon, we study the response of a neutron star to two types of perturbations to the vortex array that threads the superfluid interior. Both mechanisms produce acceptable fits to glitch observations in the four pulsars we study. The two models make different predictions for the generation of internal heat and subsequent enhancement of surface emission. Future glitch observations coordinated with surface emission measurements will play a key role in distinguishing between the two glitch models we investigate.

CHAPTER 1

INTRODUCTION

Neutron Stars: Creation and Discovery

Neutron stars are a product of the continuously evolving Universe. Gas clouds gather to form new stars which shine by fusing fundamental elements, beginning with hydrogen and continuing up to iron for the highest mass stars. The end of a star's life brings a recycling of the gas that created it, now rich with heavier elements, along with a compact remnant which is left behind to join the stellar graveyard.

Neutron stars, together with white dwarfs and black holes, make up the population of stellar remnants in the Universe. Although the mass distribution of the progenitor population is not yet known in detail, in general low mass stars ($M \lesssim 8M_\odot$, where $M_\odot$ is the mass of our Sun) evolve into white dwarfs, higher mass stars ($8M_\odot \lesssim M \lesssim 25M_\odot$) evolve into neutron stars, and the highest mass stars ($M \gtrsim 25M_\odot$) create black holes (Ergma & van den Heuvel 1998). The closest known neutron star is 200 light years from Earth[1] (Walter 2000); beyond it our Galaxy alone contains at least 10 million neutron stars according to current estimates. A neutron star is a compact, extraordinarily dense star having a mass $M \simeq 1.4M_\odot$, a radius $R \simeq 10$ km, and a strong magnetic field $10^{12} \lesssim B \lesssim 10^{14}$ G (inferred from dipole spin-down of the star)[2]. A neutron star is supported by the pressure of degenerate fermions (neutrons

[1]This neutron star is designated RX J185635-3754

[2]Compare this to the Earth's magnetic field of $B_\oplus \simeq 0.5$ G.

and electrons). The average density of a neutron star is approximately twice that of nuclear density (where nuclear density is $\rho_o \simeq 2.8 \times 10^{14}$ g cm^{-3}). Most of the nuclei in the stellar interior are dissociated into their constituent particles (neutrons, protons and electrons). At such high densities, the equilibrium state of the matter is about 90% neutrons by mass. The density of a neutron star is similar to that of a nucleus, but overall, the star is a macroscopic environment of ultra-dense matter, unlike anything studied on Earth.

Neutron stars found their place in theoretical astrophysics long before they were observed. Baade and Zwicky (1934) introduced the term *neutron star* when they suggested that a supernova results from the evolution of a main-sequence star into a remnant composed primarily of neutrons[3]. Oppenheimer and Volkoff (1939) derived the general relativistic equations which describe the internal structure of a neutron star. Migdal (1959) originally suggested that the interior of such stars would be superfluid. Despite obvious interest in these remarkable objects, neutron star research remained firmly in the theoretical arena, since it was believed that neutron stars would be difficult, if not impossible, to detect. This situation changed, however, in 1967 with the first discovery of a radio pulsar[4] by graduate student Jocelyn Bell and her advisor Anthony Hewish at the Jodrell Bank Observatory in Manchester, England (Hewish et al. 1968). This discovery earned Hewish and fellow radio astronomer Martin Ryle the Nobel Prize in Physics in 1974. In the months surrounding Bell's observation of periodic radio pulses, Pacini (1967) and Gold (1968) suggested that

[3]The neutron itself had only been recently discovered by Chadwick in 1932.
[4]This radio pulsar now bears the designation PSR 1919+21.

the pulsations could be produced by a rapidly rotating, magnetized neutron star. Further observations have confirmed this basic picture. The term *pulsar* is now used to describe a rotating neutron star which has a pulsed electromagnetic radiation signature.

Neutron stars have many manifestations. In rotation-powered pulsars, the type discovered by Jocelyn Bell, the star's magnetic field converts rotational energy into electromagnetic radiation. This process slows the star's rotation rate over time. The radiation signal appears pulsed as the star's rotation sweeps the radiation beam across our line of sight. Neutron stars in binary systems can accrete matter from a companion; the matter surrounds the neutron star in a gaseous disk. These accretion-powered pulsars convert the gravitational potential energy of the accreted matter into photons. These systems can produce low-luminosity x-ray emission as well as strong x-ray bursts. The discovery of the first *magnetar* occurred in 1998 (Kouveliotou et al. 1998). Magnetars are rotating neutron stars which have extremely high magnetic fields ($B \simeq 10^{14}$ G), and exhibit a variety of energetic phenomena that are probably driven by decay of their intense magnetic fields. Anomalous x-ray pulsars (AXP's) are slowly rotating neutron stars which exhibit strong x-ray emission. Soft gamma repeaters (SGR's) are observed to emit multiple, intense bursts of low-energy gamma-rays, and are thought to be rotating neutron stars as well. AXP's and SGR's are probably two observational manifestations of magnetars. The work in this thesis will focus on isolated, rotation-powered pulsars, which we discuss in more detail next.

Neutron Stars: Structure

Because of their small size and great distance from Earth, astronomers have yet to resolve an isolated neutron star into an observable disk which can be imaged and studied. Physical parameters such as the mass and radius must be determined indirectly. In 1974, Rhodes and Ruffini placed theoretical limits $0.2M_{\odot} \lesssim M \lesssim 3.5M_{\odot}$ on the mass required to gravitationally bind a neutron star. Considerable progress has been made in the determination of the mass by observing neutron stars in binary systems. Measurements and upper limits of the masses of 14 binary systems which contain at least one neutron star are presented in Figure 1. In these cases, study of the orbital dynamics has provided mass determinations which span a remarkably narrow range, with a mass of $M \simeq 1.4M_{\odot}$ being in agreement with all the data (Thorsett & Chakrabarty 1999). Observational values for neutron star radii have been obtained by fitting thermal emission measurements with blackbody radiation spectra and atmospheric models. These measurements yield neutron star radii of 8 - 15 km. Theoretically, neutron star radii can be calculated after assuming a mass for the star and an equation of state of the interior. The exact equation of state for neutron star matter is unknown, mostly due to uncertainties in nucleon-nucleon interactions above nuclear density. Equations of state differ above nuclear density. Soft equations of state (e.g., Baym, Pethick & Sutherland 1971), for which the matter is relatively compressible, predict a radius of $R \simeq 8$ km for a $1.4M_{\odot}$ star. Stiff equations of state (e.g., Pandharipande & Smith 1975), for which the matter has relatively low compressibility, predict $R \simeq 15$ km, for the same mass. The work in

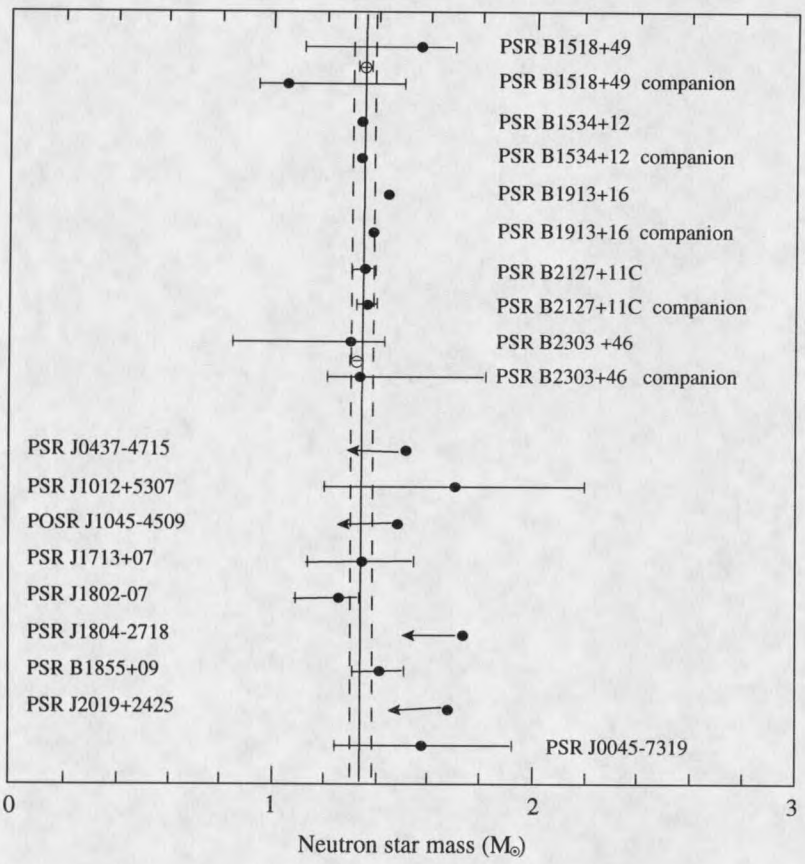

Figure 1. Neutron star masses from observations of radio pulsar systems. Five double neutron star systems are shown at the top of the diagram. In two cases, the average neutron star mass in a system is known with much better accuracy than the individual masses; these average masses are indicated with open circles. Eight neutron star white dwarf binaries are shown in the center of the diagram, and one neutron star-main-sequence star binary is shown at bottom. Vertical lines are drawn at $M = 1.35 \pm 0.04 M_{\odot}$, the range which is consistent with all measurements (from Thorsett & Chakrabarty 1999).

this thesis uses the medium equation of state of Friedman & Pandharipande (1981). Future determinations of the mass-radius relationship in neutron stars promise to constrain the equation of state of nuclear matter in a way not currently possible in terrestrial laboratories.

Equation of state calculations also provide models for the physical state of neutron

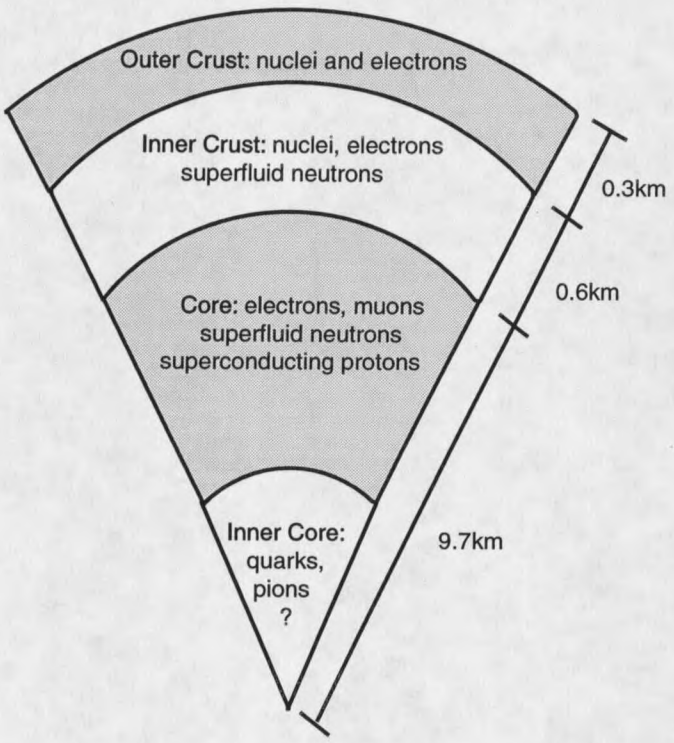

Figure 2. The internal structure of a $1.4M_{\odot}$ neutron star. Dimensions are representative of a star with a moderate equation of state.

star matter as a function of density. The current view of the neutron star interior consists of several distinct layers (Fig. 2). These layers include the atmosphere, the outer and inner crust, and the core. Below the thin atmosphere (of thickness less than 1 cm; Miller 1992), lies a solid outer crust. The outer crust consists of a lattice of neutron-rich nuclei, immersed in a relativistic, degenerate electron gas. Above a density of $\sim 4.3 \times 10^{11}$ g cm^{-3}, the *neutron drip* density, nuclei coexist with a neutron liquid and degenerate electrons. The inner crust extends from neutron drip to near nuclear density. The nuclei become more neutron-rich with increasing density, having mass numbers of several hundred near nuclear density. Neutrons in

the inner crust are believed to be in superfluid form. Superfluidity is a phenomenon that occurs when bosons condense into their ground state. Systems of fermions can condense into a superfluid if they can form Cooper pairs. In neutron star matter, pairing occurs through the strong force to form n-n and p-p paired states. Neutrons in the inner crust can pair in a singlet $^1S_0$ state. In the core, both neutrons and protons can form a superfluid, with the proton superfluid being superconducting due to the proton charge. Neutrons in the core pair in a triplet $^3P_2$ state, while the protons are in a $^1S_0$ state. Cooper pairing occurs when the temperature falls below a critical temperature. Calculations of critical temperatures for these pairing states, as functions of density, give $T_{\rm crit} \simeq 10^9 - 10^{10}$ K (e.g., Ainsworth, Pines & Wambach 1989; Wambach, Ainsworth & Pines 1991). The core consists mostly of superfluid neutrons with a few percent superconducting protons, normal electrons and muons. The inner core may contain exotic matter such as quarks, pions or kaons.

A pure superfluid has macroscopic occupation of the ground state. Such a system flows without friction, and cannot rotate as a whole. However, when the superfluid is in a container which is rotating above a critical rotation rate, it is thermodynamically favorable for the superfluid to rotate as well. Superfluid rotation is achieved by the formation of an array of vortex lines within which the fluid is normal. This phenomenon is observed in rotating He II in terrestrial laboratories (see, e.g.Yarmchuk & Packard 1982). At the rotation rate of a typical neutron star, the superfluid is also rotating and contains $\sim 10^{17}$ vortices, which will be discussed in Chapter 3. Friction associated with the normal fluid in the vortex cores generates heat and exerts torque

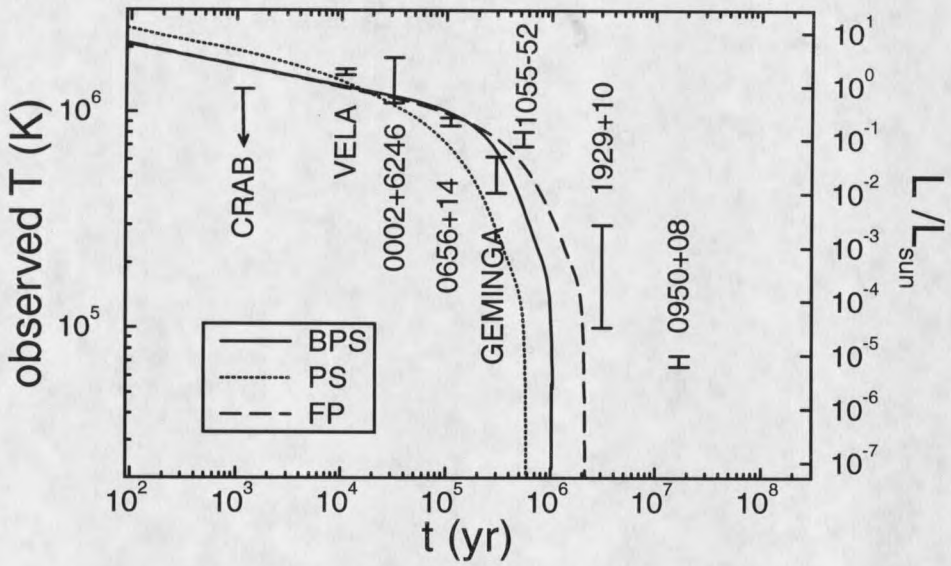

Figure 3. Neutron star thermal evolution, observations and cooling curves. Standard cooling curves are shown for stars with $M = 1.4M_{\odot}$ for three different equations of state: PS (Pandharipande & Smith 1975), FP (Friedman & Pandharipande 1981) and BPS (Baym, Pethick & Sutherland 1971). Cooling simulations are from Van Riper (1991). Observational measurements (and one upper limit) are also indicated. See Tables 2 and 3 of Chapter 2 for references to the observational data.

on the crust. The thermal evolution and rotational dynamics of a neutron star are affected by the rotation of the superfluid interior. The observable consequences of superfluidity in neutron stars are the focus of this thesis.

Neutron Stars: Cooling

Unlike main sequence stars, neutron stars are no longer undergoing nuclear fusion. A neutron star can be thought of as a hot ember, which looses heat to its surrounding over time. Since the 1980's, space-based x-ray telescopes have made observations of the thermal emission from neutron star surfaces possible. By observing neutron stars of different ages, a picture of how a neutron star cools with time has been assembled (see Tsuruta 1998 for a comprehensive review). Figure 3 shows observational measurements and upper limits for eight neutron stars, with several theoretical cooling predictions for different equations of state.

When a neutron star is formed during a supernova explosion, its internal temperature is approximately 10^{11} K. Neutrino emission processes quickly cool the star to below $T \simeq 10^{10}$ K, on a timescale of about a day. A neutron star becomes isothermal within $\sim 10^4$ yrs after its birth (Van Riper 1991; Umeda et al.1993). Neutrino emission dominates the cooling until the internal temperature falls below $T \simeq 10^8$ K, corresponding to a surface temperature of $T_{\rm obs} \simeq 10^6$ K, at an age of approximately $t_{\rm age} \simeq 10^5$ years. At this stage photon cooling from the surface becomes more important than neutrino losses.

How quickly a neutron star cools depends on the equation of state, relevant cooling processes, and possible internal heat sources. Constraints can be placed on physical processes within the star by making comparisons between thermal observations and theoretical cooling models. For standard cooling models the dominant neutrino

cooling process in the core is the modified URCA[5] process. The reaction is:

$$n + n \rightarrow n + p + e^- + \bar{\nu}_e$$

$$n + p + e^- \rightarrow n + n + \nu_e. \qquad (1.1)$$

If the proton fraction in the core is high ($\gtrsim$14%), neutrino cooling occurs via the much faster direct URCA process (see, e.g.Prakash 1994). In the crust, the dominant neutrino cooling process occurs by electron-ion bremsstrahlung, the scattering of relativistic electrons with nuclei. Energy loss through photon cooling at the surface of the star occurs essentially as blackbody radiation (modified by the atmospheric composition). Cooling rates are presented in detail in Chapter 3.

Comparison of cooling models with thermal observations indicate that older neutron stars are heated (see Fig. 3). PSR 1929+10 and PSR 0950+08, have significantly higher temperatures than the cooling calculations can explain. Chapter 2 will investigate a promising internal heat source that can explain this puzzle.

Neutron Stars: Spin Behavior

Typical radio pulsar rotation periods lie between several milliseconds and several seconds. Isolated radio pulsars are observed to spin down at remarkably steady rates. The accuracy and predictability of the spin period increase has distinguished radio pulsars as 'the most accurate clocks in the Universe'.

Many pulsars have been observed to experience sudden spin-ups, or *glitches*, on top of their steady spin-down. Glitches produce fractional changes in rotation rate

[5]The URCA reaction, which is a sink for the star's energy, gets its name from the URCA casino in Rio de Janeiro, which is a sink for money.

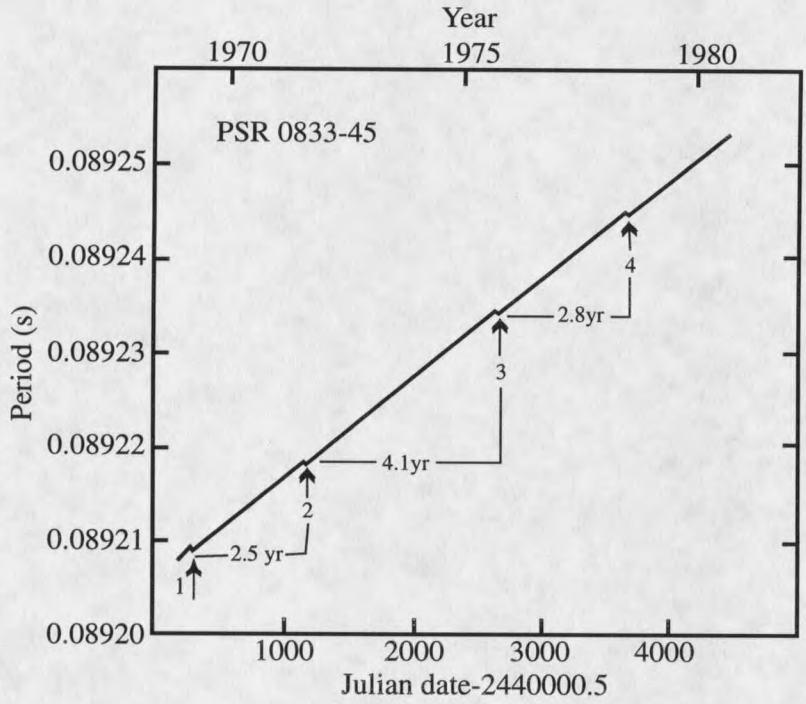

Figure 4. The pulse period of PSR 0833-45 (Vela) from late 1968 to 1980. The secular period increase is due to steady spin down of the star by the electromagnetic torque. The four large jumps are enumerated (from Downs 1981).

$(\Delta\nu/\nu)$ from 10^{-10} to 10^{-6} (where ν is the rotational frequency of the pulsar). An example of four glitches in the Vela pulsar is shown in Figure 4. Despite the small fractional change in rotation rate, glitches involve enormous changes in rotational energy of up to $\simeq 10^{43}$ ergs. Glitches have been seen to repeat in many pulsars, with some evidence for occurrence at regularly-spaced intervals (Link, Epstein & Lattimer 1999). Since the first glitch observation in the Vela pulsar (Radhakrishnan & Manchester 1969; Reichley & Downs 1969) numerous theories have been proposed to explain the glitch phenomenon. It was first suggested that the sudden spin up was due

to abrupt relaxation of the star's oblateness[6], thus reducing the moment of inertia and increasing the rotation rate of the crust (Ruderman 1969). This readjustment might occur after a starquake, which would crack the solid crust. However, comparisons with glitch observations indicate that this model cannot accommodate the frequency and relative size of these events (Alpar & Baykal 1994). Most current theories ascribe glitches to variable coupling between the stellar crust and superfluid interior. To date, a single theory of pulsar glitches which can encompass all the aspects of glitch behavior has yet to be proposed. Chapter 3 will investigate possible explanations for the glitch phenomenon.

Plan of this Thesis

This thesis addresses observational consequences of superfluidity on the thermal evolution and rotational dynamics of isolated neutron stars. Differential rotation of the star's liquid interior generates heat. The coupling between the liquid interior and the solid crust (which affects the star's rotation rate) is temperature dependent. Thus, the thermal and rotational dynamics of a neutron star are coupled and must be considered together. Chapter 2 demonstrates that frictional heat generated between the solid and liquid components of the star can account for the unexpectedly high surface temperatures in older neutrons stars ($t_{\rm age} \simeq 10^6$ yrs). Interpreting the observed temperatures as due to frictional heat provides limits on the strength of frictional coupling between the neutron star crust and the superfluid it contains, a

[6]Due to their rapid rotation, neutron stars are expected to have a slightly oblate shape. For a polar diameter of 20 km, the equatorial diameter would be approximately 1 m larger.

parameter which is difficult to obtain from first principles.

Numerical simulations of pulsar glitches are presented in Chapter 3 in an effort to distinguish between two different types of glitch theories. We obtain good fits to glitch observations in the four pulsars we study for both types of theories. We also present simulations of the thermal pulse generated during a glitch, which could be visible from the stellar surface months to years after the glitch occurs. Diagnostics are needed to distinguish between different glitch theories. Such diagnostics are provided by the magnitude and the timing of the thermal emission, which differs between the two glitch mechanisms we study. Future thermal emission measurements coordinated with spin observations will help constrain the glitch theories presented in Chapter 3. Chapter 4 provides a summary of this work.

CHAPTER 2

LATE-TIME THERMAL EVOLUTION

Introduction

A cooling neutron star cools initially through neutrino emission before making a transition to photon cooling at an age of $\sim 10^5$ yrs (see, e.g., Tsuruta 1998; see Fig. 5). Internal heating processes, if they occur, could affect when and how abruptly the star makes the transition to photon cooling. Later, when the heating power begins to exceed the luminosity from residual heat, the heat source would control the star's thermal evolution. Internal heating processes that could occur include superfluid frictional heating (see, e.g., Greenstein 1975; Harding, Guyer, & Greenstein 1978; Alpar et al. 1987; Shibazaki & Lamb 1989; Van Riper, Epstein, & Miller 1991; Umeda et al. 1993; Van Riper, Link & Epstein 1995), structural readjustment through plastic flow or "starquakes" (Baym & Pines 1971; Ruderman 1976; Cheng et al. 1992), chemical disequilibrium driven by the star's spin-down (Reisenegger 1995), and magnetic field decay (Thompson & Duncan 1996; Heyl & Kulkarni 1998). Temperature measurements of neutron stars older than $\sim 10^5$ yrs provide strong tests of cooling models in the photon cooling era, and offer the possibility of constraining the heating processes that might occur. In particular, the recent temperature measurements of PSRs 1929+10 and 0950+08 by Pavlov, Stringfellow & Córdova (1996) pose a serious challenge to standard cooling models, and seem in fact to demand internal heating

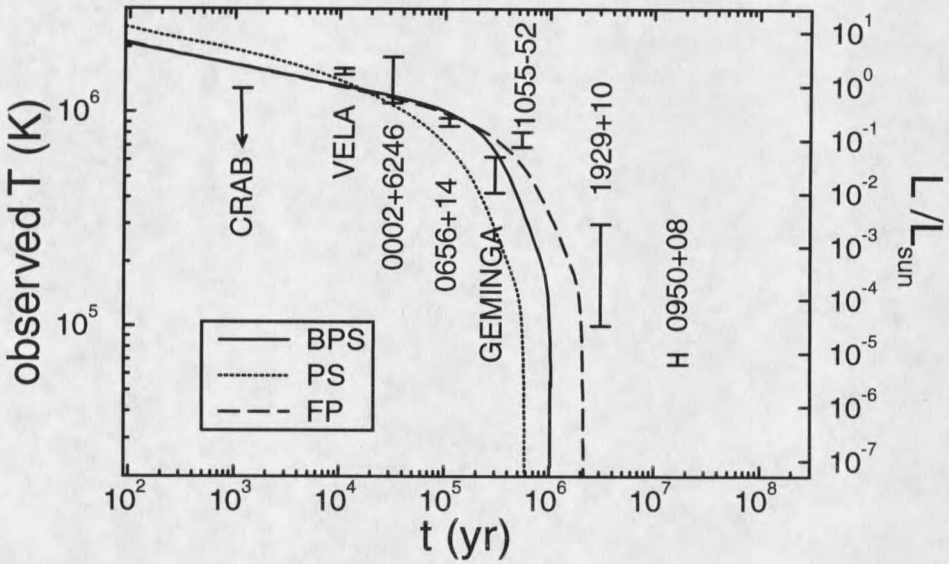

Figure 5. Thermal evolution curves for three different equations of state. FP (Friedman & Pandharipande 1981), PS (Pandharipande & Smith 1975) and BPS (baym, Pethick, & Sutherland 1971) equations of state are shown. These simulations do not include internal heating. Shown are surface temperatures and luminosities measured by a distant observer. The observational temperature determinations and the conversion to luminosity assume a stellar mass of 1.4 $M_\odot$ and radius $R = 10$ km.

at rates of $\sim 10^{-4} L_\odot$ and $\sim 10^{-5} L_\odot$, respectively (see Fig. 5).

The work presented in this chapter has been published in The Astrophysical Journal (Larson & Link 1999). In this chapter we explore the possibility that heat generated by friction between the neutron star crust and the interior neutron fluid is the dominant heating processes taking place in old neutron stars with conventional

magnetic fields ($\sim 10^{12}$ G). Most of the mass of a neutron star is expected to be in the form of a neutron superfluid that condenses shortly after the star's birth (Migdal 1959). Large velocity differences between the superfluid and the crust could develop in the star's inner crust, where the vortices that thread the rotating superfluid pin to nuclei (Anderson & Itoh 1975; Ruderman 1976; Alpar 1977; Epstein & Baym 1988; Pizzochero, Viverit, & Broglia 1997). Differential rotation between the stellar crust and the superfluid would lead to frictional heat generation, while variations in the frictional coupling would affect the star's spin behavior. Studies of superfluid friction in the inner crust indicate that the coupling can be highly temperature-dependent, scaling with temperature as $e^{-E/kT}$, where E is an energy $\gg kT$ (see, e.g., Alpar et al. 1984; Link, Epstein & Baym 1993, hereafter Link, Epstein & Baym 1993; Chau & Cheng 1993). The star's thermal and rotational evolution are thus coupled and must be considered together. Usually the core superfluid is regarded as corotating with the stellar crust (Alpar, Langer & Sauls 1984), though Sedrakian & Sedrakian (1995; see also Sedrakian & Cordes 1999) have suggested that interactions between superfluid vorticity in the core with the London current near the crust-core interface could maintain differential rotation between the crust and core. In this case, friction between the core superfluid and the normal matter could also be a heat source.

The goal of this chapter is to describe the role played by superfluid friction in late-time neutron star thermal evolution. Although heat generation in the core is a possibility, we will focus primarily on friction in the crust, as the coupling there has been studied in detail. We consider first the case in which the superfluid is

in rotational equilibrium, spinning down at the same rate as the crust. This case was originally considered by Alpar et al. (1987) and applied to the upper limit on the luminosity of PSR 1929+10 available at the time to obtain a constraint on the excess angular momentum residing in the superfluid. In later work, Shibazaki & Lamb (1989), Umeda et al. (1993), and Van Riper, Link & Epstein (1995) included the effects of superfluid friction in simulations of neutron star thermal evolution to obtain further constraints on the heating through this process. This study is largely motivated by the recent measurements of the temperatures of the old pulsars PSRs 1929+10 and 0950+08 (Pavlov, Stringfellow & Córdova 1996), which, as we show, provide the most stringent constraints to date on the rotation of the superfluid interior.

A crucial issue in neutron star thermal evolution is the possible development of thermal instabilities. Shibazaki and Mochizuki (1994) have shown that under certain circumstances a feedback instability between the star's thermal and rotational states can occur if the frictional coupling of the superfluid to the crust is sufficiently sensitive to temperature; as heat is generated, the frictional coupling is increased, creating more heat. The instability continues until the star heats to a temperature at which it is stable. In this manner, the star executes a limit cycle in which its temperature oscillates about the temperature at which it is marginally stable, accompanied by oscillations in the rotation rate. This case we study in detail. We conclude that the coupling of the superfluid to the crust is nearly independent of temperature in a star older than $\sim 10^6$ yrs, effectively decoupling the star's rotational and thermal evolution. We use x-ray and optical data from cooling neutron stars to obtain constraints

on the excess angular momentum residing in the superfluid.

Candidate Heating Processes in Old Pulsars

Fig. 5 shows a comparison of thermal evolution calculations (neglecting possible internal heating) with the surface temperature measurements of eight neutron stars. Residual heat is adequate to explain the temperatures of the younger objects, but cannot account for the temperatures of PSR 1929+10 and PSR 0950+08. Pavlov, Stringfellow & Córdova (1996) have measured temperatures of $T_{s,\infty} = 1.0 - 3.0 \times 10^5$ K for PSR 1929+10 and $6.6 - 7.4 \times 10^4$ K for PSR 0950+08 (see below for further discussion of the observations). The discrepancy between these measurements and the predictions of cooling theory is far too large to be accounted for by atmospheric uncertainties or modification of the energy transport by a magnetic field, and internal heating is required. We now discuss several candidate heating processes: superfluid friction, structural relaxation, chemical disequilibrium and magnetic field decay.

Differential rotation between the neutron star crust and the neutron superfluid would generate heat through friction. If the superfluid and crust are in rotational equilibrium with respect to each other (both slowing down at the same rate), the heating power is (Alpar et al. 1984; Shibazaki & Lamb 1989; Van Riper, Link & Epstein 1995; Umeda et al. 1993; see eq. 2.8 below)

$$H(t) = \Delta J_s \left|\dot{\Omega}_0\right| \equiv I_s \bar{\omega} \left|\dot{\Omega}_0\right|, \tag{2.1}$$

where $\Delta J_s \equiv I_s \bar{\omega}$ is the excess angular momentum residing in the superfluid, I_s is the moment of inertia of the portion of the superfluid that is differentially rotating,

$\bar{\omega}$ is the angular velocity difference between the two components averaged over the superfluid moment of inertia and $|\dot{\Omega}_0|$ is the spin-down rate. In principle, the heat could be generated anywhere in the star in which there are superfluid neutrons. Usually, however, the superfluid in the core is regarded as tightly coupled to the rotation of the solid crust through the spontaneous magnetization of neutron vortex lines by superconducting proton currents (Alpar, Langer & Sauls 1984). Analyses of glitch data (Chau et al. 1993; Abney, Epstein, & Olinto 1996) and spin variations in accreting neutron stars (Boynton et al. 1984; Baykal, Alpar, & Kızıloğlu 1991; Baykal 1997) and in isolated pulsars (Boynton 1981; Deeter 1981) support this picture. In the inner crust, however, interaction between crustal nuclei and superfluid vorticity could lead to substantial differential rotation (see, e.g., Anderson & Itoh 1975) and heating. The velocity difference that can develop is determined by uncertain microphysics, however, $\bar{\omega}$ could exceed ~ 10 rad s^{-1} (Epstein & Baym 1988; Pizzochero et al. 1997). In a star with a stiff equation of state and a thick crust, ΔJ_s could then be as large as $\sim 6 \times 10^{45}$ ergs s, in which case the heating power is approximately

$$H(t) = 0.8 \left(\frac{\Delta J_s}{6 \times 10^{45} \text{ ergs s}} \right) \left(\frac{P}{0.2 \text{ s}} \right)^{-1} \left(\frac{t_{\text{age}}}{10^6 \text{ yr}} \right)^{-1} L_\odot, \qquad (2.2)$$

where P is the star's spin period, t_{age} is the spindown age $\equiv P/2\dot{P}$, and a rapid initial spin rate was assumed. A heating rate this large would begin to play an important role in thermal evolution after $\sim 10^5$ yrs, when $H(t)$ becomes comparable to the luminosity from residual heat.

Another process that heats the star is structural relaxation occurring as the star spins down and becomes less oblate. The neutron star crust probably becomes brittle

when its temperature drops below $\sim 10^8$ K (Ruderman 1976) at an age of $\sim 10^4$ yrs, and subsequently suffers structural relaxation through violent starquakes. The rate of heat generation is then of order (Cheng et al. 1992),

$$\dot{E}_{\rm quake} \sim \frac{\mu\theta_c^2}{t_{\rm age}} = 10^{-5} \left(\frac{\mu}{10^{48}\ {\rm erg}}\right) \left(\frac{\theta_c}{10^{-3}}\right)^2 \left(\frac{t_{\rm age}}{10^6\ {\rm yr}}\right)^{-1} L_\odot, \qquad (2.3)$$

where μ is the shear modulus of the crust and θ_c is the critical strain angle at which the crust breaks. The critical strain angle is quite uncertain. Cheng et al. (1992) have shown that structural relaxation could constitute an important heat source in older stars if θ_c is $\gtrsim 10^{-2}$. However, a value of θ_c this large is close to that for a perfect Coulomb lattice, while lattice imperfections could make θ_c considerably smaller (Smolukowski 1970). We assume that superfluid friction dominates starquake heating.

Reisenegger (1995) has studied heating arising as a neutron star spins down and compression of the matter drives it from chemical equilibrium. For the $\sim 10^{12}$ G fields expected for most isolated neutron stars this process appears to be relatively unimportant, but could be relevant in stars with small magnetic fields ($\lesssim 10^{10}$ G). Reisenegger cautions, however, that chemical disequilibrium in superfluid neutron matter could give larger heating rates than those he estimates for normal matter.

Thompson & Duncan (1996) have studied heat generation by the decay of a strong magnetic field, and argue that the dominant decay process of a $\gtrsim 10^{14}$ G field is the irrotational mode of ambipolar diffusion (Goldreich & Reisenegger 1992). Equating the rate of energy loss by field decay to the photon luminosity gives a surface

temperature of

$$4\pi\sigma R^2 T_s^4 \simeq \left(\frac{4\pi R^3}{3}\right)\left(\frac{B^2}{8\pi t_{ambip}^{irr}}\right) \tag{2.4}$$

where B is the field strength and

$$t_{ambip}^{irr} \simeq \frac{5\times 10^{15}}{T_8^6 B_{12}^2}\text{yr}. \tag{2.5}$$

Relating the surface temperature to the internal temperature using the results of Gudmundsson, Pethick & Epstein (1982; see eq. 2.49 below) we obtain

$$T_s = 5.8\times 10^5 \left(\frac{B}{10^{16}\text{G}}\right)^{-0.57}. \tag{2.6}$$

The fields required to account for the observed temperatures of PSRs 1929+10 and 0950+08 are $\sim 10^{16}$ G and $\sim 10^{17}$ G, respectively. By contrast, the *dipole* fields of these objects inferred from the vacuum dipole model are only $\sim 10^{11}$ G. Thus, heating by magnetic field decay appears an unlikely heat source to power the emission of PSRs 1929+10 and 0950+08.

Steady Heating From Superfluid Friction

The first situation we consider is internal heating arising from steady slow-down of the neutron superfluid. In the next section, we study perturbations to this equilibrium state.

We describe a neutron star as consisting of two components - a solid crust and an interior liquid (the superfluid). The crust is acted upon by an external torque, and the crust and superfluid are coupled through friction. Regardless of the system's initial

spin state, eventually an equilibrium will be reached in which the two components are both spinning down at the same rate, with the liquid spinning more rapidly than the solid to a degree determined by the external torque and the strength of the frictional coupling. In this state of rotational equilibrium, friction between the two components generates heat at a rate that is nearly constant (for an external torque that is changing slowly).

The rate of heat production is given by the difference between the rate of change of the total rotational energy of the star and the rate at which work is done by the external torque (Alpar et al. 1984; Shibazaki & Lamb 1989; Van Riper, Link & Epstein 1995):

$$\begin{aligned} H(t) &= N_{ext}\Omega_c(t) - \frac{d}{dt}\left[\frac{1}{2}I_c\Omega_c^2(t) + \frac{1}{2}\int dI_s\,\Omega_s^2(\mathbf{r},t)\right] \\ &= \int dI_s|\dot{\Omega}_s(\mathbf{r},t)|\omega(\mathbf{r},t), \end{aligned} \tag{2.7}$$

where N_{ext} is the external braking torque, $\Omega_c(t)$ is the angular velocity of the crust and any components of the star tightly coupled to it, $\Omega_s(\mathbf{r},t)$ is the superfluid angular velocity at position $\mathbf{r}$ in the star, $\omega(\mathbf{r},t) \equiv \Omega_s(\mathbf{r},t) - \Omega_c(t)$ is the angular velocity *lag* between the superfluid and the crust, and I_s is the superfluid moment of inertia. Equation 2.7 gives the heating rate whether the two components are in rotational equilibrium or not. In rotational equilibrium, the crust superfluid is everywhere spinning down at the rate of the crust $|\dot{\Omega}_0(t)|$, and the heating rate is

$$H = \Delta J_s|\dot{\Omega}_0(t)|, \tag{2.8}$$

where $\Delta J_s \equiv \int dI_s\omega_0(\mathbf{r},t)$ is the excess angular momentum in the superfluid and

$\omega_0(\mathbf{r},t)$ is the lag in equilibrium. After $\sim 10^6$ yrs, when the star has lost most of its residual heat, the heating rate is approximately balanced by cooling through the emission of surface photons, i.e.,

$$4\pi\sigma R_\infty^2 T_{s,\infty}^4 = \Delta J_s |\dot{\Omega}_{0,\infty}(t)|, \tag{2.9}$$

where R_∞ is the radius, $T_{s,\infty}$ is the surface temperature and $|\dot{\Omega}_{0,\infty}(t)|$ is the spin-down rate (subscript ∞ indicates quantities seen by a distant observer; ΔJ_s is evaluated at the stellar surface). Observed stellar quantities are related to their values at the surface through the redshift $e^{-\Phi} \equiv (1-2GM/Rc^2)^{-1/2}$ as

$$T_{s,\infty} = e^{\Phi} T_s \qquad |\dot{\Omega}_{0,\infty}(t)| = e^{2\Phi}|\dot{\Omega}_0(t)| \qquad R_\infty = e^{-\Phi} R. \tag{2.10}$$

Later, we will apply equation 2.9 to PSRs 1929+10 and 0950+08 to obtain estimates for the values of ΔJ_s required to heat these sources to their observed temperatures.

Thermal-rotational Instability

We now study the stability of the rotational equilibrium described above by determining how a neutron star containing a pinned inner crust superfluid responds to a perturbation of its thermal and rotational state. This problem was originally considered by Shibazaki & Mochizuki (1994) under the simplifying assumption that the superfluid angular velocity has no gradients. We extend their work to account for gradients in the superfluid angular velocity lag (as would arise from vortex pinning) and the effects of quantum tunneling and vortex self-energy on the superfluid dynamics. We find (as did Shibazaki & Mochizuki 1994) that under some circumstances a feedback instability that couples the star's thermal and rotational states

can occur. In contrast to Shibazaki & Mochizuki (1994) however, we find that the thermal-rotational instability cannot occur in stars older than $\sim 10^6$ yrs. While our discussion will be formulated with coupling to the inner crust superfluid in mind, many of our results are general and can be applied to coupling with a core liquid.

Perturbation Analysis

The star's total angular momentum changes under an external torque as (neglecting general relativistic effects)

$$\dot{J}_{\rm tot}(t) = I_c\dot{\Omega}_c(t) + \int dI_s\,\dot{\Omega}_s(\mathbf{r},t) = N_{\rm ext}(t) \equiv -I|\dot{\Omega}_0(t)|, \tag{2.11}$$

where I_c is the moment of inertia of the crust plus any other component(s) to which it is effectively coupled (e.g., the core), I_s is the superfluid component in differential rotation, and $I \equiv I_c + I_s$ is the total moment of inertia of the neutron star. In rotational equilibrium, the crust superfluid, the crust and the core are all spinning down at a rate $|\dot{\Omega}_0(t)|$.

A neutron star becomes isothermal within $\sim 10^4$ yrs after its birth (Van Riper 1991; Umeda et al. 1993). The star's thermal evolution is then governed by

$$C_v\dot{T}(t) = H + \Lambda_c, \tag{2.12}$$

where T is the internal temperature, C_v is the heat capacity, H is the internal heating rate and Λ_c is the cooling rate. The star cools through emission processes that depend on age and composition. We parameterize the cooling rate as

$$\Lambda_c = -BT^n(t), \tag{2.13}$$

where B and n are constants which depend on the cooling mechanism. For the first $\sim 10^5$ yrs of a neutron star's thermal evolution, the dominant mode of energy loss is through modified ($n = 8$) or direct ($n = 6$) URCA reactions. Later, the star cools primary through the emission of photons from the surface ($n \simeq 2.2$). Combining equation 2.8 for the equilibrium heating rate with equations 2.12 and 2.13 gives the temperature evolution equation for the equilibrium state:

$$C_{v,0}\dot{T}_0 = -BT_0^n + \Delta J_s|\dot{\Omega}_0(t)|, \tag{2.14}$$

where here and henceforth the subscript "0" denotes equilibrium quantities, themselves functions of time.

The heating rate in equation 2.7 is determined by the rotational state of the superfluid. The superfluid obeys the equation of motion (Baym & Chandler 1983),

$$\frac{\partial \mathbf{w}(\mathbf{r},t)}{\partial t} + \nabla \times [\mathbf{w}(\mathbf{r},t) \times \mathbf{v}_v(\mathbf{r},t)] = 0, \tag{2.15}$$

where $\mathbf{w} \equiv \nabla \times \mathbf{v}_s$ is the superfluid vorticity, $\mathbf{v}_s$ is the fluid velocity and $\mathbf{v}_v$ is the vortex velocity. All quantities are averaged over regions containing many vortices. The circulation around any contour is given by

$$\oint d\mathbf{l} \cdot \mathbf{v}_s = \int_A d\mathbf{A} \cdot \mathbf{w} = \kappa N, \tag{2.16}$$

where N is the number of vortices surrounded by the contour of area A and κ is the quantum of circulation ($h/2m_n$; m_n = neutron mass). The component of the vorticity along the axis of rotation is related to the areal density n of vortices in the perpendicular plane. For rotation along the z-axis, equation 2.16 gives

$$\mathrm{w}_z(\mathbf{r},t) = \kappa n(\mathbf{r},t). \tag{2.17}$$

The $z-$component of equation 2.15 gives the conservation law

$$\frac{\partial n(\mathbf{r},t)}{\partial t} + \nabla \cdot [n(\mathbf{r},t)\mathbf{v}_v(\mathbf{r},t)] = 0. \tag{2.18}$$

We shall focus on axisymmetric superfluid rotation. In this case the z-component Ω_s of the superfluid angular velocity a distance r_p from the rotation axis is given by

$$\oint d\mathbf{l} \cdot \mathbf{v}_s = 2\pi r_p^2 \Omega_s(\mathbf{r},t) = \kappa \int_0^{r_p} dr_p' \, 2\pi r_p' n(\mathbf{r},t). \tag{2.19}$$

From equation 2.18, the equation of motion is

$$\dot{\Omega}_s(\mathbf{r},t) = -\frac{w_z}{r_p} v(\omega,T) = -v_{cr}(\omega,T)\left(\frac{2}{r_p} + \frac{\partial}{\partial r_p}\right)\Omega_s(\mathbf{r},t), \tag{2.20}$$

where $v_{cr}(\omega,T)$, the average radial velocity of vortex lines, is determined by the microscopic processes that govern the vortex mobility. In the absence of pinning, the superfluid would approximate rigid body rotation so that $\partial\Omega_s/\partial r_p \simeq 0$. For simplicity, we assume that pinning introduces gradients in Ω_s that are negligible compared to $2\Omega_s/r_p$.

We assume that thermal conduction maintains isothermality and neglect gradients in the perturbed temperature. We examine the response of the system to the following *axisymmetric* perturbations of its thermal and rotational states:

$$\Omega_s(\mathbf{r},t) = \Omega_{s,0}(\mathbf{r}) + \delta\Omega_s(\mathbf{r},t) \tag{2.21}$$

$$\Omega_c(t) = \Omega_{c,0} + \delta\Omega_c(t) \tag{2.22}$$

$$\omega(\mathbf{r},t) = \omega_0(\mathbf{r}) + \delta\omega(\mathbf{r},t) \tag{2.23}$$

$$T(t) = T_0 + \delta T(t), \tag{2.24}$$

where unperturbed quantities are evaluated at the time of the initial perturbation and $|\dot{\Omega}_{s,0}| = |\dot{\Omega}_{c,0}| = |\dot{\Omega}_0|$. Equation 2.11 becomes

$$I_c \delta\dot{\Omega}_c(t) + \int dI_s \, \delta\dot{\Omega}_s(\mathbf{r}, t) = 0. \tag{2.25}$$

To linear order in the perturbations, equation 2.12 becomes the following integro-differential equation:

$$\begin{aligned} C_{v,0}\delta\dot{T}(t) = -C_{v,0}\frac{\dot{T}_0}{T_0}\delta T(t) \quad &- \quad BnT_0^{n-1}\delta T(t) \\ &+ \quad |\dot{\Omega}_0| \int dI_s \delta\omega(\mathbf{r}, t) - \int dI_s \omega_0(\mathbf{r}) \delta\dot{\Omega}_s(\mathbf{r}, t). \end{aligned} \tag{2.26}$$

Equation 2.20 becomes

$$\delta\dot{\Omega}_s(\mathbf{r}, t) = -|\dot{\Omega}_0| \left(\eta_\omega \frac{\delta\omega(\mathbf{r}, t)}{\omega_0(\mathbf{r})} + \eta_T \frac{\delta T(t)}{T_0} + \frac{\delta\Omega_s(\mathbf{r}, t)}{\Omega_{s,0}(\mathbf{r})} \right), \tag{2.27}$$

where

$$\eta_\omega = \frac{\partial \ln v}{\partial \ln \omega} \qquad \eta_T = \frac{\partial \ln v}{\partial \ln T}, \tag{2.28}$$

are evaluated in equilibrium and measure the sensitivity of the vortex radial velocity to changes in the lag and temperature. The quantities η_ω and η_T could have spatial dependence, but for the vortex velocity we will adopt below they are nearly constant.

We seek separable solutions for the perturbed quantities of the form $\delta A(\mathbf{r}, t) = \delta A(\mathbf{r}) e^{-i\omega t}$. Combining equations 2.25 - 2.27, we obtain

$$\begin{aligned} &i\omega \left[\frac{\eta_\omega \eta_T}{T_0} I_0^2 + \frac{\eta_T I_c}{T_0} I_1 - C_{v,0}\eta_\omega I_{-1} - \frac{\eta_\omega \eta_T}{T_0} I_1 I_{-1} + I_c C_{v,0} \right] - C_{v,0} I_c \frac{\dot{T}_0}{T_0} \\ - \quad &BnT_0^{n-1} I_c + \frac{|\dot{\Omega}_0| I \eta_T}{T_0} I_0 + \frac{C_{v,0}\dot{T}_0 \eta_\omega}{T_0} I_{-1} + BnT_0^{n-1}\eta_\omega I_{-1} = 0, \end{aligned} \tag{2.29}$$

where

$$I_n \equiv \int dI_s \omega_0^n(\mathbf{r}) \left(\frac{i\omega}{|\dot{\Omega}_0|} - \frac{\eta_\omega}{\omega_0(\mathbf{r})} - \frac{1}{\Omega_{s,0}(\mathbf{r})} \right)^{-1} \tag{2.30}$$

Evaluation of equation 2.29 requires a form for $\omega_0(\mathbf{r})$. Pinning calculations indicate that the pinning energy per nucleus peaks near a density of $\sim 10^{14}$ g cm^{-3} (Epstein & Baym 1988; Pizzochero et al. 1997); in these regions, ω_0 will be the largest. To model this behavior, we treat ω_0 as taking a value $\omega_0 = \omega_{0,\max}$ through a region of total moment of inertia $\Delta I_s < I_s$, and zero otherwise. Since the pinning energy is largest in the densest regions of the crust, ΔI_s probably accounts for most of the crustal superfluid's moment of inertia. Evaluating the integrals in equation 2.29, we find,

$$\omega^2 + i\omega Y - Z = 0, \tag{2.31}$$

with

$$Y = \frac{\dot{T}_0}{T_0} + \frac{BnT_0^{n-1}}{C_{v,0}} + \tilde{\Omega} - \frac{|\dot{\Omega}_0|\eta_T \omega_{0,\max} \Delta I_s}{C_{v,0} T_0}, \tag{2.32}$$

$$Z = \left(\frac{\dot{T}_0}{T_0} + \frac{BnT_0^{n-1}}{C_{v,0}} \right) \tilde{\Omega} + \frac{\eta_T |\dot{\Omega}_0^2| I \Delta I_s}{C_{v,0} T_0 I_c}, \tag{2.33}$$

where

$$\tilde{\Omega} \equiv |\dot{\Omega}_{s,0}| \left(\frac{1}{\Omega_0} + \frac{(I_c + \Delta I_s)\eta_\omega}{I_c \omega_{0,\max}} \right). \tag{2.34}$$

Perturbations are damped when $Y > 0$, unstable when $Y < 0$, and marginally stable (or oscillatory) when $Y = 0$. The condition for a star to be unstable is,

$$\frac{\dot{T}_0}{T_0} + \frac{BnT_0^{n-1}}{C_{v,0}} + \tilde{\Omega} - \frac{|\dot{\Omega}_0|\eta_T \omega_{0,\max} \Delta I_s}{C_{v,0} T_0} \leq 0. \tag{2.35}$$

Using the equilibrium equation (eq. 2.14) we make the replacement

$$BT_0^n = |\dot{\Omega}_0|\Delta I_s \omega_{0,\max} - C_{v,0}\dot{T}_0, \tag{2.36}$$

to obtain a quadratic equation for the critical temperature T_c,

$$T_c^2 + \frac{(n-1)I_c\omega_{0,\max}|\dot{T}|}{\eta_\omega I|\dot{\Omega}_0|}T_c + \frac{(n-\eta_T)I_c\omega_{0,\max}^2\Delta I_s}{aI\eta_\omega} = 0, \tag{2.37}$$

where $a \equiv C_{v,0}/T_0$ is independent of temperature for degenerate matter. We have assumed $\tilde{\Omega} \sim |\dot{\Omega}_0|\eta_\omega I/\omega_{0,\max}I_c$, which is valid as long as $\omega_{0,\max} \ll \eta_\omega\Omega_s$. Equation 2.37 has a positive solution:

$$T_c = -\frac{(n-1)\omega_{0,\max}I_c|\dot{T}|}{2\eta_\omega I|\dot{\Omega}_0|} + \frac{1}{2}\left(\frac{(n-1)^2\omega_{0,\max}^2I_c^2|\dot{T}|^2}{\eta_\omega^2 I^2|\dot{\Omega}_0|^2} + \frac{4(\eta_T-n)\omega_{0,\max}^2I_c\Delta I_s}{a\eta_\omega I}\right)^{1/2}. \tag{2.38}$$

Below we estimate $\eta_T = \eta_\omega \simeq 30$. For a star of age $\sim 10^4$ yrs, $|\dot{T}|$ is $\sim 10^{-7}$K s^{-1} and $|\dot{\Omega}_0|$ is $\sim 10^{-10}$rad s^{-2}. Taking $\omega_{0,\max} \sim 10$ rad s^{-1} and $n = 8$ (modified URCA cooling), we see that the first term under the square root is negligible compared to the second. The critical temperature is thus approximately

$$T_c^2 \simeq \frac{(\eta_T-n)\omega_{0,\max}^2I_c\Delta I_s}{a\eta_\omega I}. \tag{2.39}$$

From equation 2.39, we see that a minimum sensitivity of the vortex velocity to temperature is required for a thermal-rotational instability to occur; for $\eta_T < n$, the star is stable at any temperature. Equation 2.39 agrees with equation 24 of Shibazaki & Mochizuki (1994) in the limit $\Delta I_s = I_s$, $\eta_T \gg n$ and $I_c \simeq I$.

Equation 2.39 can be applied for any coupling of the superfluid and crust that depends on T and ω. In principle, the superfluid component with excess angular

momentum $\omega_{0,\max}\Delta I_s$ could be anywhere in the star. In the inner crust, however, pinning of vortices to the nuclear lattice (Anderson & Itoh 1975; Ruderman 1976; Alpar 1977; Epstein & Baym 1988; Pizzochero et al. 1997) could sustain significant differential rotation between the superfluid and the crust. The mobility of vortices in the presence of pinning determines the superfluid's ability to respond to changes in temperature and rotation rate. Vortex dynamics in the presence of pinning has been studied in detail by Link & Epstein (1991) and Link, Epstein & Baym (1993) under the assumption that vortex stresses do not break the nuclear lattice. We now review the key results of their work, and study the implications of vortex pinning for the thermal-rotational instability.

Vortex Dynamics in the Presence of Pinning

Were superfluid vortices perfectly pinned to the inner crust lattice, the superfluid velocity would be fixed. As the solid crust slows under the external torque, a velocity difference between the crust and superfluid would develop exerting a Magnus force on the pinned vortices directed radially outward. If the lag ω locally exceeds a critical value ω_c, vortices cannot remain pinned in the presence of the Magnus force; the vortices unpin and flow outward, spinning down the superfluid. The critical lag is determined by the condition that the Magnus force per unit length of vortex equal the pinning force per unit length (see, e.g., Link & Epstein 1991)

$$\frac{F_p}{l} = \rho_s \kappa r_p \omega_c, \tag{2.40}$$

where F_p is the pinning force per nucleus, l is the lattice spacing and ρ_s is the superfluid mass density.

For $\omega < \omega_c$, pinned vortices can still move outward as thermal or quantum excitations allow them to overcome their pinning barriers. The resulting average velocity of *vortex creep* is determined by the pinning strength, the properties of vortices, the characteristic energy of excitations on a pinned vortex, and the velocity difference between a pinned vortex and the superfluid flowing past it. Accounting for quantum effects and the vortex self-energy, Link, Epstein & Baym (1993) and Link & Epstein (1991) obtain a creep velocity of the form (see eq. 6.9 of Link, Epstein & Baym 1993)

$$v_{cr} = v_0 \exp(-E_a(\omega)/T_{\rm eff}). \tag{2.41}$$

Here E_a is the *activation energy* for a segment of vortex line to overcome its pinning barrier; it decreases with ω, becoming zero for $\omega = \omega_c$. The prefactor v_0 is a microscopic velocity comparable to the radial component of the velocity of an unpinned vortex segment. The radial velocity is determined by the dissipative processes associated with vortex motion. Epstein & Baym (1992) have shown that drag arising from the excitation of Kelvin modes causes free vortices to move radially outward at velocities comparable to the velocity difference between the superfluid and normal matter. For the pinning energies estimated by Epstein & Baym (1988), this velocity difference could be $\sim 10^6$ cm s^{-1}; we estimate $v_0 \simeq 10^6$ cm s^{-1}. The effective temperature, $T_{\rm eff}$, is (eq. 4.10, Link, Epstein & Baym 1993)

$$T_{\rm eff} = T_q \coth \frac{T_q}{T}, \tag{2.42}$$

where T_q is the *cross-over temperature* that determines the transition from vortex motion through thermal activation to quantum tunneling. For $T \gg T_q$, vortices move primarily through classical thermal activation. For $T \ll T_q$, the dominant process is quantum tunneling. In these two limits

$$T_{\rm eff} \rightarrow \begin{cases} T & \text{for } T \gg T_q \text{ (classical)} \\ T_q & \text{for } T \ll T_q \text{ (quantum)} \end{cases} \tag{2.43}$$

In equilibrium, the superfluid and the crust are both spinning down at a rate $|\dot{\Omega}_0(t)|$. From equations 2.20 and 2.41, the equilibrium state satisfies

$$\frac{E_a(\omega_0)}{T_{\rm eff}} = \ln \frac{4 v_0 t_{\rm age}}{r_p}, \tag{2.44}$$

where we took $\Omega_s/|\dot{\Omega}_0| \simeq 2t_{\rm age}$. The pinning force is a function of density alone, and so is constant on spherical shells. From equation 2.44, we see that ω_0 is nearly constant on such shells except near the rotational poles. For purposes of obtaining estimates, we henceforth take $r_p \simeq R$. For $v_0 = 10^6$ cm s^{-1} and $t_{\rm age} = 10^6$ yrs,

$$\ln \frac{4 v_0 t_{\rm age}}{R} \simeq 30. \tag{2.45}$$

In equilibrium, $E_a(\omega_0)$ must take a particular local value for given $T_{\rm eff}$ and $t_{\rm age}$. The value of the steady state lag is determined by the critical lag, $T_{\rm eff}$ and $t_{\rm age}$. If the pinning strength is relatively large, ω_0 must be $\simeq \omega_c$ to ensure that the vortices can overcome their pinning barriers and creep at the required steady-state rate. We refer to this case of vortex creep near the critical lag as *strongly-driven.* On the other hand, if the pinning force per nucleus is relatively small, ω_0 must be $\ll \omega_c$ to ensure that the vortices do not creep too quickly. We refer to this case as *weakly-driven.*

[These cases correspond to the limits of *flexible* and *stiff* vortices discussed by Link & Epstein (1991), and *non-linear* and *linear* creep in Alpar, Cheng & Pines 1989]. In the equilibrium state we have assumed, the local lag has everywhere adjusted to the value required to satisfy equation 2.44.

Evaluated about equilibrium, the sensitivity of the vortex velocity in equation 2.41 to temperature is

$$\eta_T = \left[\ln \frac{4v_0 t_{\rm age}}{R}\right] \left(\frac{T_q}{T}\right)^2 \operatorname{csch}^2 \frac{T_q}{T}. \tag{2.46}$$

In the classical limit ($T \gg T_q$), $\eta_T \simeq 30$. Below $T = T_q$, both η_T and T_c quickly drop to zero as T is reduced. Hence, for the limit cycle to be relevant, $T \gtrsim T_q$ is required.

The cross-over temperature T_q is equal to half the ground state energy of excitations on a pinned vortex line, and depends sensitively on the pinning energy and density. For weakly-driven vortices, Link, Epstein & Baym (1993) estimate (eq. 3.11 Link, Epstein & Baym 1993)

$$T_q \simeq 0.2 \left(\frac{\Lambda}{3}\right) \left(\frac{l}{50 \text{ fm}}\right)^{-2} \text{ keV}, \tag{2.47}$$

where Λ is a weak function of density and we have chosen fiducial values appropriate to the denser regions of the inner crust. At lower density, e.g., near the neutron drip density, Λ is $\simeq 7$.

For strongly-driven vortices, pinning drives the ground state energy of vortex excitations up to a considerably higher value (eq. 3.13, Link, Epstein & Baym 1993):

$$T_q \simeq 60 \left(\frac{\Lambda}{3}\right) \left(\frac{l}{50 \text{ fm}}\right)^{-2} \text{ keV}. \tag{2.48}$$

To compare these temperatures to those of cooling neutron stars, we convert from surface temperature to internal temperature using the results of Gudmundsson, Pethick & Epstein (1982):

$$T_8 = 1.288 \left(\frac{T_{s,6}^4}{g_{s,14}} \right)^{0.455} \tag{2.49}$$

where

$$g_s = \frac{GM}{R^2} e^{-\Phi}. \tag{2.50}$$

Here $T_8 \equiv T/10^8$ K, $T_{s,6} \equiv T_s/10^6$ K, $g_{s,14} \equiv g_s/10^{14}$ cm s^{-2} is the surface gravity, and $T_{s,\infty} = e^{\Phi} T_s$. For typical neutron star parameters, the internal temperature is

$$T = 12 \; T_{s,6,\infty}^{1.82} \text{ keV}. \tag{2.51}$$

For PSR 0950+08, we estimate 0.09 keV $< T <$ 0.11 keV. This object is thus well into the quantum creep regime, for which $\eta_T \simeq 0$. The limit cycle cannot occur, and steady slowdown of the crust and superfluid is a stable state. Our conclusion regarding the stability of old stars differs from that of Shibazaki & Mochizuki (1994), who assumed that thermal creep is always the dominant process.

For PSR 1929+10 the case is less clear; we find 0.18 keV $< T <$ 1.3 keV, compared to $T_q \simeq 0.2$ keV estimated in equation 2.47. However, this estimate applies only to the special case of extremely stiff vortices; T_q could be substantially higher than 0.2 keV. It thus appears that PSR 1929+10 is also in the quantum creep regime (or borderline), undergoing steady slow-down.

Stars younger than PSR 1929+10 ($t_{\rm age} = 3 \times 10^6$ yrs), could be in the thermal creep regime, and hence could be subject to the thermal-rotational instability. Such

a star becomes unstable if the temperature falls below the critical temperature given by equation 2.39. The quantity η_ω, which measures the sensitivity of the creep rate to changes in ω is, from equations 2.41 and 2.44,

$$\eta_\omega = -\left[\ln \frac{4v_0 t_{\rm age}}{R}\right] \frac{d\ln E_a}{d\ln \omega}. \tag{2.52}$$

The form for $E_a(\omega)$ depends on the strength of pinning. In the weakly- and strongly-driven limits, the activation energy is (eq. B.12, Link & Epstein 1991, in the limit $\omega \ll \omega_c$; eq. 3.15, Link & Epstein 1991)

$$E_a(\omega) \rightarrow \begin{cases} \frac{\beta}{\omega} & \text{weakly-driven} \\ U_0(1-\frac{\omega}{\omega_c})^{3/2} & \text{strongly-driven,} \end{cases} \tag{2.53}$$

where U_0 is the pinning energy per nucleus, and β is a parameter that measures the strength of the coupling and is related to U_0. For strongly-driven vortices, U_0 is relatively large ($\gtrsim$ 1 MeV), and T_q is up to $\sim$ 60 keV. A neutron star is expected to cool below this temperature within $\sim$ 100 years of its birth. For strongly-driven vortices, therefore, quantum tunneling is the dominant creep process during most of the star's thermal evolution, and the thermal-rotational instability cannot occur. Hence, the weakly-driven case is the relevant one for the thermal-rotational instability. In this case

$$\eta_\omega = \ln \frac{4v_0 t_{\rm age}}{R} \simeq 30. \tag{2.54}$$

Taking $\eta_T = \eta_\omega \simeq 30$, we estimate the internal temperature at which the star becomes unstable from equation 2.39. In the limit $I_s \ll I_c$, appropriate if it is the inner crust

Table 1. Neutron Star Parameters based on the equation of state of Friedman & Pandharipande (1981).

M ($M_\odot$)	1.4
R (km)	10.9
$e^{-\Phi}$	1.27
I_s (g cm^2)	7.3×10^{43}
a (ergs K^{-2})	3.3×10^{29}

superfluid that drives the instability, we obtain

$$T_c = 11 \left(\frac{a}{3.3 \times 10^{29} \text{ergs K}^{-2}} \right)^{-1/2} \left(\frac{\omega_{0,\max}}{10 \text{ rad s}^{-1}} \right) \left(\frac{\Delta I_s}{7.3 \times 10^{43} \text{ g cm}^2} \right)^{1/2} \text{keV}, \tag{2.55}$$

where $n = 8$ for modified URCA cooling in a young neutron star. Here and in the following, we estimate stellar parameters such as I_s, R and a using a $1.4 M_\odot$ stellar model based on the Friedman & Pandharipande (1981) equation of state (see Table 1). A cooling neutron star reaches a temperature of ~ 10 keV after $\sim 10^4$ yrs. While the critical temperature depends sensitively on the uncertain pinning parameters $\omega_{0,\max}$ and ΔI_s, this estimate suggests that young, cooling neutron stars *could* be unstable to perturbations in temperature and rotation rate. If, on the other hand, $\omega_{0,\max}$ or ΔI_s are significantly smaller than estimated in equation 2.55, the star will cool into the quantum creep regime before it can become unstable. As a star cools and reaches its critical temperature, temperature perturbations begin to grow. Stability is restored as the star is heated to slightly above its critical temperature. The star is again able to cool, eventually becoming unstable again. A limit cycle ensues, wherein the star oscillates about its T_c as originally demonstrated by Shibazaki & Mochizuki (1994).

To evaluate the characteristic period of the oscillations about this marginally-stable state, we solve equation 2.31 with $Y = 0$. Using equation 2.14 and assuming $I_s \ll I_c$, we obtain

$$\tau_{osc} \simeq 2\pi \left[\frac{\eta_T(1+\eta_\omega)(n-1)BT_0^{n-1}|\dot{\Omega}_0|}{aT_0(\eta_T-1)\omega_{0,\max}} + \frac{\eta_\omega(\eta_T+\eta_\omega)|\dot{\Omega}_0|^2}{(\eta_T-1)\omega_{0,\max}^2} \right]^{-1/2}. \tag{2.56}$$

For a young star cooling through the modified URCA process, the first term is negligible for $\omega_{0,\max} \simeq 1 - 10$ rad s^{-1}. Taking $\eta_T = \eta_\omega = 30$, $\Omega_{s,0}/|\dot{\Omega}_0| \simeq 2t_{age}$ and the spin period as $P \simeq 2\pi/\Omega_{s,0}$ gives

$$\tau_{osc} \simeq 0.26 \left(\frac{P}{0.1 \text{ s}}\right) \left(\frac{\omega_{0,\max}}{10 \text{ rad s}^{-1}}\right) t_{age}. \tag{2.57}$$

Constraints from Surface Temperature Measurements

Old Pulsars

Pavlov, Stringfellow & Córdova (1996) have recently detected thermal emission from PSRs 1929+10 and 0950+08 in the UV-optical band using the COSTAR corrected Faint Object Camera on the Hubble Space Telescope. Assuming the observed flux arises from the entire surface of a neutron star with radius 10 km, they obtain surface temperatures of $T_s^\infty = 1.0 - 3.0 \times 10^5$ K for PSR 1929+10 and $6.6 - 7.4 \times 10^4$ K for PSR 0950+08. Previous X-ray observations of PSRs 1929+10 (Yancopoulos, Hamilton, & Helfand, 1994) and 0950+08 (Manning & Willmore, 1994) produced blackbody fits for emitting regions of only $\sim$ 20-30 meters in diameter, suggesting that the observed X-ray emission originates from a hot polar cap. However, for both

Table 2. Pinning Constraints for Old Stars.

Pulsar	$\log t_{\rm age}$ (yrs)	$\log T_{s,\infty}$ (K)	$\lvert\dot{\Omega}_{0,\infty}\rvert$ (rad s^{-2})	ΔJ_s (ergs s)	$\bar{\omega}$ (rad s^{-1})
1929+10	6.49	5.00 - 5.48	1.4×10^{-13}	9.8×10^{41} - 8.1×10^{43}	0.01 - 1.1 [1]
0950+08	7.23	4.82 - 4.87	2.3×10^{-14}	1.1×10^{42} - 1.8×10^{42}	0.01 - 0.02
1055-52	5.73	5.84 - 5.91	9.4×10^{-13}	3.3×10^{44} - 6.3×10^{44}	4.6 - 8.6

[1] Uncertainties in the values of ΔJ_s and $\bar{\omega}$ arise from uncertainties in the surface temperature

of these objects, extension of the blackbody spectra into the UV-optical range predicts a flux which is several orders of magnitude smaller than that observed by Pavlov, Stringfellow & Córdova (1996), consistent with the interpretation that the UV-optical emission originates from the entire neutron star surface.

The previous analysis indicates that these two sources are too cold for the thermal-rotational instability to occur. Assuming steady heating by superfluid friction, we determine from equation 2.9 the values of the excess angular momentum ΔJ_s and average lag $\bar{\omega} \equiv \Delta J_s / I_s$ required to heat these objects to their observed temperatures. We find $\Delta J_s \sim 4 \times 10^{43}$ ergs s and $\bar{\omega} \sim 0.6$ rad s^{-1} for PSR 1929+10, and $\Delta J_s \sim 1 \times 10^{42}$ ergs s and $\bar{\omega} \sim 0.02$ rad s^{-1} for PSR 0950+08 (see Table 2). Our estimates were obtained for an FP equation of state, which gives a radius $R \simeq 11$ km, close to that assumed for the surface temperature determinations. Our results are consistent with earlier upper limits on $\bar{\omega}$ obtained for PSR 1929+10. Shibazaki & Lamb (1989) obtained $\bar{\omega} < 0.02$ rad s^{-1} and $\bar{\omega} < 4.0$ rad s^{-1} for stiff and soft equations of state. Alpar et al. (1987) found $\bar{\omega} < 0.7$ rad s^{-1} for a moderate equation of state.

Some amount of internal heating also appears to be required for PSR 1055-52 (see

Fig. 5). Ögelman & Finley (1993) obtained a temperature of $T_s^\infty = 6.9{-}8.1{\times}10^5$ K for this pulsar using ROSAT PSPC data. This temperature was obtained by interpreting the soft blackbody component of the spectrum as originating from a cooling neutron star of radius $\simeq$ 10 km. If we assume that steady heating by the internal superfluid provides all of the photon luminosity for this pulsar, we obtain $\Delta J_s \sim 5 \times 10^{44}$ ergs s and $\overline{\omega} \sim 7$ rad s^{-1}.

Young Pulsars

Surface temperature measurements and upper limits for young pulsars are given in Table 3, all fits are blackbody fits with a stellar radius of 10 km. These pulsars could be subject to the thermal-rotational instability discussed above. We consider PSR 1055-52 along with the younger pulsars because its internal temperature is high enough that the limit cycle cannot be ruled out. For most neutron stars younger than $\sim 10^6$ yrs, the observed temperatures can be accounted for by their residual heat content. As previously discussed, if the thermal-rotational instability occurs, a cooling neutron star cannot cool below its critical temperature. By requiring the internal temperature deduced from the observed surface temperature to be greater than or equal to the critical temperature, we obtain from equation 2.39 the constraint,

$$4.1 \times 10^4 \left(\frac{(\eta_T - \dot{n})\omega_{0,\max}^2 \Delta I_s}{a \eta_\omega R^{1.82} e^{-2.73\Phi}} \right)^{0.275} \leq T_{s,\infty}, \tag{2.58}$$

giving an upper limit on $\omega_{0,\max}^2 \Delta I_s$ inasmuch as R, Φ, η_T, $\dot{a}$ and n are known.

Superfluid pinning is expected to be strongest in the densest regions of the inner crust; the characteristic lag $\omega_0(\mathbf{r})$ will be largest in these regions. It is reasonable to

Table 3. Pinning Constraints for Young Stars.

Pulsar	$\log t_{\rm age}$ (yrs)	$\log T_{s,\infty}$ (K)	$\omega_{0,\rm max}^2 \Delta I_s$ (ergs)	$\bar{\omega}^{\diamond}$ (rad s^{-1})	References
0531+21	3.10	< 6.19	$< 5.2 \times 10^{46}$	< 35	Becker & Aschenbach (1995)
0833-45	4.05	6.20	$< 5.4 \times 10^{46}$	< 36	Ögelman et al. (1993)[1]
0002+6246	4.50	6.26	$< 8.9 \times 10^{46}$	< 46	Hailey & Craig (1995)[2]
0656+14	5.04	5.97	$< 7.7 \times 10^{45}$	< 14	Finley et al. (1992)
0630+178	5.48	5.80	$< 1.8 \times 10^{45}$	< 6.6	Halpern & Ruderman (1993)
1055-52	5.73	5.91	$< 3.6 \times 10^{45}$	< 9.3	Ögelman & Finley (1993)

$^{\diamond}$ The upper limits on $\bar{\omega}$ assume $\bar{\omega} < \omega_{0,\rm max}$ as expected for most models of pinning.

[1] The blackbody fits yield stellar radii of 2-4 km.

[2] The blackbody fits yield stellar radii of 2-4 km.

expect then that $\omega_{0,\rm max} > \bar{\omega} \equiv I_s^{-1} \Delta J_s$. For this situation, we obtain the constraint,

$$\bar{\omega} \leq \left(\frac{\omega_{0,\rm max}^2 \Delta I_s}{I_s} \right)^{1/2} . \tag{2.59}$$

where $\omega_{0,\rm max}^2 \Delta I_s$ is obtained with equation 2.58. For stars younger than $\sim 10^5$ yrs, the dominant cooling process is neutrino emission; we assume $n = 8$ (modified URCA process). We take $\eta_T = \eta_\omega = 30$, as estimated above, and the stellar parameters of Table 1 for R, Φ and a. In Table 3 we list constraints from equations 2.58 and 2.59 for young neutron stars. We obtain upper limits on $\bar{\omega}$ of ~ 30 rad s^{-1}, typically. Note that these constraints apply *only* if the dominant creep process is classical thermal activation; if quantum tunneling is the dominant process, the star is stable at any temperature.

Discussion

PSRs 1929+10 and 0950+08 require significant internal heating to account for their observed temperatures. A promising candidate heat source is friction between the neutron star crust and the superfluid it contains. We have studied the effects of superfluid friction on the long-term thermal and rotational evolution of a neutron star. We conclude that average differential rotation between the superfluid and the crust of $\bar{\omega} \sim 0.6$ rad s^{-1} and ~ 0.02 rad s^{-1} would account for the temperatures of PSRs 1929+10 and 0950+08 respectively. A larger lag, $\bar{\omega} \sim 7$ rad s^{-1}, is compatible with the temperature of PSR 1055-52 if its luminosity is supplied mostly by superfluid friction. These differential velocities could be sustained by the pinning of superfluid vortices to the inner crust lattice.

Pinned vortices can creep outward through thermal fluctuations or quantum tunneling, depending on the pinning strength and stellar temperature. For thermally-activated creep, the coupling between the superfluid and crust is highly sensitive to temperature. Under some circumstances, a feedback instability can occur that brings the superfluid and crust closer to corotation and heats the star until stability is restored. A hysteresis develops in which the star oscillates about its critical temperature. For stars older than $\sim 10^6$ yrs, however, vortex creep occurs through quantum tunneling, and the creep velocity is too insensitive to temperature for a thermal-rotational instability to occur; these stars are stable. Our conclusion regarding the stability of old stars differs from that of Shibazaki & Mochizuki (1994), who assumed that thermal creep is always the dominant process. The thermal-rotational

instability could, however, occur in younger stars. Assuming that young stars are stable or marginally stable leads to upper limits on the superfluid differential velocity of ~ 30 rad s^{-1}. These upper limits are consistent with the estimates for $\bar{\omega}$ obtained for the older PSRs 1929+10 and 0950+08.

The estimates we obtain for $\bar{\omega}$ are consistent with first-principles calculations of the maximum lag sustainable by vortices before unpinning. Based on the pinning calculations of Alpar, Cheng & Pines (1989) and Ainsworth, Pines & Wambach (1989), Van Riper, Link & Epstein (1995) obtain an upper limit to the average lag velocity of $\bar{\omega} \sim 10$ rad s^{-1}. From the pinning calculations of Epstein & Baym (1988), Van Riper, Link & Epstein (1995) obtain an upper limit of $\bar{\omega} \sim 10^2$ rad s^{-1}. The recent calculations of Pizzochero, Viverit & Broglia (1997) give a pinning force of $F_p = 0.63$ MeV fm^{-1} at a density $\rho_s = 8 \times 10^{13}$ g cm^{-3}, and a pinning energy of 7.5 MeV; the corresponding critical lag is $\omega_c = 16$ rad s^{-1}.

To estimate the pinning strength required to sustain differential rotation of the magnitudes estimated above, we take F_p appearing in equation 2.40 to be U_0/r_0, where r_0 is the effective range of the pinning potential. With the lag from PSR 1929+10 we obtain,

$$U_0 \gtrsim 0.5\,\mathrm{MeV}\left(\frac{\bar{\omega}}{0.6\ \mathrm{rad\ s^{-1}}}\right)\left(\frac{\rho_s}{10^{14}\ \mathrm{g\ cm^{-3}}}\right)\left(\frac{R}{10\ \mathrm{km}}\right)\left(\frac{r_0}{10\ \mathrm{fm}}\right)\left(\frac{l}{50\ \mathrm{fm}}\right). \quad (2.60)$$

Equation 2.60 represents a lower limit since $\bar{\omega} < \bar{\omega}_c$, however, $\bar{\omega}$ could be close to $\bar{\omega}_c$ for pinning strengths this large (Link, Epstein & Baym 1993). Our estimates of $\bar{\omega}$ for PSR 0950+08 imply a pinning energy $\gtrsim 0.02$ MeV.

The thermal-rotational instability described in this chapter might produce oscillations in the temperature and spin-down rate of younger pulsars with a characteristic period of $\sim 0.3\ t_{\rm age}$. Oscillations in the Crab pulsar, for example, could occur over a timescale of $\tau_{osc} \sim 10^2$ yrs. Detection of such long-period oscillations, especially in the presence of timing irregularities (e.g., glitches), would be problematic. Observational evidence for the thermal-rotational instability in any neutron star would offer valuable insight into the manner in which the neutron star crust is coupled to its superfluid interior.

Our estimates for the excess angular momentum ΔJ_s required to heat PSRs 1929+10 and 0950+08 to their observed temperatures hold whether the frictional heat is generated in the crust or in the core. In obtaining constraints on the average lag $\bar{\omega}$, we assumed coupling to the inner crust superfluid. If the coupling is in the core (e.g. Sedrakian & Sedrakian 1995), these estimates scale as $\Delta J_s/I_s$, where I_s is the moment of inertia of the component that possesses differential rotation. The upper limits on $\Delta I_s \omega_{0,\rm max}^2$ obtained for young pulsars apply for the crust since the coupling parameters η_T and η_ω were determined for vortex creep.

An issue that complicates all interpretations of surface temperatures from cooling neutron stars is the uncertainty in atmospheric composition. We used the results of blackbody fits in our analysis. Temperature measurements are also available for several pulsars using model atmospheres. Heavy-element atmospheric models produce temperatures similar to the blackbody results. However, non-magnetic, light-element atmospheres can give temperatures up to three times lower than those obtained with

blackbody fits (Romani 1987). If the temperature were in fact three times lower than the blackbody value, $\bar{\omega}$ estimated for PSRs 1929+10, 0950+08 and 1055-52 would decrease by almost two orders of magnitude. The upper limits on $\bar{\omega}$ obtained for younger stars would decrease by a factor of three. Hence, the results presented in this chapter are conservative and could decrease with improved atmospheric considerations and temperature measurements.

Sudden increases in pulsar rotation rates (*glitches*) have been observed in many younger pulsars and are thought to represent angular momentum transfer from the superfluid to the crust. In the Vela pulsar, for example, fractional changes in the rotation rate of the crust of $\sim 10^{-6}$ are observed every few years (Cordes, Downs, & Krause-Polstorff 1988). The maximum angular momentum available for a glitch is ΔJ_s, giving a maximum glitch magnitude of

$$\frac{\Delta\Omega_c}{\Omega_c} \simeq \frac{\Delta J_s}{I_c \Omega_c} \simeq 2.6 \times 10^{-2} \left(\frac{\Delta J_s}{2 \times 10^{45} \text{ ergs s}}\right) \left(\frac{I_c}{1.1 \times 10^{45} \text{ g cm}^2}\right)^{-1} \left(\frac{\Omega_c}{70 \text{ s}^{-1}}\right)^{-1}. \tag{2.61}$$

The upper limit of $\bar{\omega} \simeq 30$ rad s^{-1} obtained for Vela gives $\Delta J_s \simeq 2 \times 10^{45}$ ergs s for the inner crust angular momentum excess, easily compatible with the angular momentum requirements of glitches. The smaller values obtained for PSRs 1929+10 and 0950+08 are also adequate to produce Vela-sized glitches, though none has been observed. In the next chapter, we turn to a detailed modeling of glitches.

CHAPTER 3

SIMULATIONS OF GLITCHES IN ISOLATED PULSARS

Introduction

Many pulsars exhibit glitches, sudden jumps in spin rate, superimposed on the gradual spin down due to electromagnetic torque (see, e.g., Lyne, Shemar & Smith 2000). Glitches involve fractional spin jumps of $\Delta\nu/\nu$ of approximately 10^{-10} to 10^{-6} with recovery to the pre-glitch spin-down rate occurring over days to months, in most cases. Some pulsars show no obvious recovery, and continue to spin down faster than had the glitch not occurred. The 1989 glitch of the Crab pulsar ($\Delta\nu/\nu \simeq 7\times10^{-8}$) was partially time-resolved (Lyne, Smith & Pritchard 1992). This glitch showed a quick rise on a timescale of hours with additional spin-up taking place over approximately one day. In contrast, the Vela "Christmas" glitch ($\Delta\nu/\nu \simeq 2 \times 10^{-6}$) observed in December of 1988 (McCulloch et al. 1990) showed much different behavior. In this case the glitch was not time-resolved, and occurred in under two minutes. The January 2000 glitch in the Vela pulsar ($\Delta\nu/\nu \simeq 3 \times 10^{-6}$), exhibited similar behavior (Dodson, McCulloch & Costa 2000). A number of pulsars (the Crab in particular) exhibit permanent increases in spin-down rate after a glitch occurs, typically $\Delta\dot{\Omega}/\dot{\Omega} \simeq 10^{-4}$. In the Crab, these offsets produce much larger cumulative timing residuals than the glitches themselves. In addition to glitches, nearly all pulsars exhibit low level fluctuations in their spin rate, timing noise, believed to be of a different origin than

glitches (see e.g., D'Alessandro et al. 1995).

Glitches are thought to represent variable coupling between the stellar crust and the superfluid interior. Two questions concerning the glitch phenomena are: 1) where in the star the coupling occurs, and, 2) how the coupling is triggered. The rotation of the neutron superfluid interior is governed by the dynamics of vortex lines; a spin jump of the crust would result from sudden motion of vortices away from the rotation axis. In the inner crust, vortices could pin to the lattice (Anderson & Itoh 1975; Alpar 1977; Alpar, Langer & Sauls 1984; Epstein & Baym 1988), allowing the superfluid to store angular momentum as the crust spins down under electromagnetic torque. The motion of vortices pinned to the crust is highly sensitive to temperature (Alpar 1977; Alpar, Cheng & Pines 1989; Link & Epstein 1991; Link, Epstein & Baym 1993; Chau & Cheng 1993a; Chau & Cheng 1993b) and a sudden deposition of heat could trigger a glitch event. Starquakes, for instance, could deposit up to $\sim 10^{42}$ ergs of heat in the crust (Baym & Pines 1971; Cheng et al. 1992). Greenstein (1979a,b) originally suggested that the sudden deposition of heat could trigger increased frictional coupling between the core superfluid and the crust, resulting in a change of the star's spin behavior. Link & Epstein (1996) have proposed a thermal glitch mechanism in which a temperature perturbation liberates pinned vortices in the inner crust from their pinning bonds, slowing the rotation rate of the superfluid, and spinning up the crust. Alternatively, Ruderman (1991) has suggested that vortex lines strongly pinned to the inner crust lattice could stress the crust to the point of fracture, allowing outward motion of vortices with plates of matter to which they are pinned. In the core, pinning

may occur between the vortices and flux tubes associated with the superconducting proton fluid (Chau, Cheng & Ding 1992), allowing the core superfluid, or a portion of it, to store angular momentum. Ruderman, Zhu & Chen (1998) have proposed a core-driven glitch mechanism in which the expanding vortex array of the core forces the magnetic flux into the highly-conductive crust, stressing it to fracture. Crust cracking allows the core vortex array to expand outward, spinning down a portion of the core superfluid and spinning up the crust. Carter, Langlois & Sedrakian (2000) have suggested that centrifugal buoyancy forces are the origin of pressure gradients sufficient to crack the crust, allowing outward vortex motion. Other possibilities include glitches which result from catastrophic unpinning of vortices in the crust (Cheng et al. 1988; Alpar & Pines 1993; Mochizuki & Izuyama 1995), and vortex motion at the crust-core boundary due to proton flux tube annihilation there (Sedrakian & Cordes 1999). In any of these crust or core-driven glitch models, dissipation that accompanies outward vortex motion generates heat that might produce detectable emission as the heat arrives at the stellar surface.

Quantitative calculations are necessary to distinguish among different models for the glitch phenomenon. The thermal glitch model of Link & Epstein (1996) produced good qualitative fits to glitch observations in the Crab and Vela pulsars. This chapter is an extension of that work with more realistic physical inputs and detailed modeling of the timing data. We include nonlinear thermal diffusion which has the effect of slowing the glitch spin-up. We also include the effects of superfluid heating due to differential rotation between the superfluid and the crust (Greenstein 1975; Harding,

Guyer & Greenstein 1978; Alpar et al. 1987; Shibazaki & Lamb 1989; Van Riper 1991; Van Riper, Epstein & Miller 1991; Umeda et al. 1993; Van Riper, Link & Epstein 1995; Larson & Link 1999) and study the propagation of heat to the stellar surface. We consider two types of rearrangement of the superfluid vortices: 1) thermal excitation of vortices over their pinning barriers (a thermal glitch) and 2) mechanical motion of vortices (a mechanical glitch). The first case models the response to sudden heating of the crust, e.g., from a starquake. The second case models catastrophic unpinning events, vortex motion as a result of crust cracking due to superfluid stresses, or core-driven glitches involving vortex motion near the crust-core boundary. In addition to simulations of the rotational dynamics, we make predictions of the thermal pulse profile which could, in some cases, be visible from the surface of the neutron star within weeks to years after a glitch occurs.

In this chapter we first provide an overview of the physical setting and discuss the treatment of the coupled rotational and thermal dynamics we use to model pulsar glitches. We then discuss the details of our numerical models. Next we present our simulations of the spin-up process and the emergence of the thermal wave at the stellar surface. We compare our simulations with spin observations of four pulsars and a thermal emission measurement following a recent glitch in the Vela pulsar. The four pulsars in our sample are those which, to date, have the best timing data surrounding their glitch events. We conclude with discussion.

Input Physics

A neutron star consists of an atmosphere, an outer and inner crust, and the core. Beneath a thin atmosphere and solid outer crust the inner crust begins at a density of $\sim 4 \times 10^{11}$ g cm^{-3} and extends to approximately nuclear saturation density, $\rho_o = 2.8 \times 10^{14}$ g cm^{-3}. The inner crust forms a neutron-rich lattice which coexists with a neutron superfluid, protons and relativistically degenerate electrons. The inner crust lattice dissolves near nuclear density (Lorenz, Ravenhall & Pethick 1993; Pethick, Ravenhall & Lorenz 1995). Most of the mass of the core is expected to reside in superfluid neutrons and superconducting protons, with electrons and muons also present.

Glitch models that rely on the superfluid interior as an angular momentum reservoir require a metastability of the vortex state to sustain differential rotation between the solid and liquid components of the star. In the inner crust the metastability could arise through pinning of vortices to the lattice. The details of pinning are uncertain. The form of the vortex-nucleus interaction potential is not well known due, in part, to uncertainties in the nucleon-nucleon interactions and the structure of the vortex core. Preliminary calculations of the vortex-nucleus interaction gave energies of $\sim$ 1-10 MeV (Epstein & Baym 1988). Pizzochero, Viverit & Broglia (1997) refined these calculations and found interaction energies on the order of several MeV per nucleus near nuclear density. By studying tension effects on the orientation of a vortex line relative to lattice axes in the inner crust, Jones (1997; 1998; 1999) has argued that

there can be significant cancellation of the pinning forces on a vortex line. The magnitude of the cancellation is determined by the extent to which a vortex line can bend to intersect pinning nuclei. These calculations were performed for a homogeneous solid lattice, but Jones (1999) has suggested that the crust could be an amorphous (heterogeneous Z) solid. The strength of vortex pinning in this situation is unknown. Given the uncertain nature of vortex pinning, we assume that pinning does occur in the inner crust, and take the effective pinning energy per nucleus to be a free parameter.

Rotational Dynamics

The total angular momentum $\mathbf{J}$ of the star is that of the *effective crust* (the crust and all components strongly coupled to it) plus the angular momentum of the superfluid,

$$\mathbf{J}_{\rm tot}(t) = I_c\mathbf{\Omega}_c(t) + \int dI_s\mathbf{\Omega}_s(\mathbf{r},t) = \mathbf{J}_0 + \mathbf{N}_{\rm ext}t, \tag{3.1}$$

where I_c is the moment of inertia of the effective crust, I_s is the crust superfluid moment of inertia and $I \equiv I_c + I_s$ is the total moment of inertia, $\mathbf{\Omega}_c$ is the angular velocity of the effective crust, and $\mathbf{\Omega}_s$ is the angular velocity of the superfluid. The initial angular momentum of the star is $\mathbf{J}_0$. The star slows under an external torque, $\mathbf{N}_{\rm ext} \equiv I\dot{\mathbf{\Omega}}_\infty(t)$. In rotational equilibrium the effective crust and the superfluid would spin down at the same rate, $-|\dot{\mathbf{\Omega}}_\infty(t)|$. The stellar core is thought to couple to the crust on timescales of less than a minute (Alpar, Langer & Sauls 1984; Abney, Epstein & Olinto 1996). We therefore take the effective crust to include the mass

of the core plus the solid crustal lattice, and the superfluid to exist between neutron drip ($\rho = 4.3 \times 10^{11}$ g cm^{-3}) and nuclear density.

We assume a geometry in which the angular momentum of the superfluid and crust are aligned with the external torque, as this is the state of lowest rotational energy for given angular momentum. The rotation rate of the inner crust superfluid is determined by the arrangement of the vortex lines which thread it. The equation of motion for the superfluid is (see Chapter 2, eq. 2.20),

$$\dot{\mathbf{\Omega}}_s(\mathbf{r},t) = -v_{cr}\left(\frac{2}{r_p} + \frac{\partial}{\partial r_p}\right)\mathbf{\Omega}_s(\mathbf{r},t), \tag{3.2}$$

where r_p is the distance from the rotation axis and v_{cr} is the average radial velocity of the vortex lines. If vortex pinning is relatively effective, as we assume, vortices can move slowly away from the rotation axis through thermal excitations or quantum tunnelling in a process of *vortex creep*.

The average velocity of vortex creep is determined by the vortex-nucleus interaction, the vortex core structure, the characteristic energy of excitations on a pinned vortex, and the velocity difference between a pinned vortex and the superfluid flowing past it. As discussed in Chapter 2 (eq. 2.41) the creep velocity has the form,

$$v_{cr} = v_0 \exp(-E_a(\omega)/T_{\rm eff}), \tag{3.3}$$

where E_a is the activation energy for a pinned vortex segment to unpin. Recall the effective temperature is $T_{\rm eff} \equiv T_q \coth\frac{T_q}{T}$, where T is the thermodynamic temperature and T_q is the crossover temperature which determines the transition from vortex motion through thermal activation to that by quantum tunnelling. The crossover

temperature depends on the ground-state excitation energy of a pinned vortex. In our simulations the stellar temperatures are much greater than the crossover temperature, so that thermal activation (classical creep) is the dominant creep mechanism. In this limit $T_{\rm eff}$ reduces to the temperature T. The multiplicative factor v_0 is comparable to the radial component of the velocity of an unpinned vortex line; we take its value to be 10^6cm s^{-1} (Link & Epstein 1991; Epstein & Baym 1992; Link, Epstein & Baym 1993).

The mechanics and energetics of unpinning are affected by the vortex self energy, or tension, $\widehat{T}$. For a vortex line with a sinusoidal perturbation of wavenumber k, the tension takes the form (Fetter 1967; see [Appendix A], Link & Epstein 1991),

$$\widehat{T} = \frac{\rho_s \kappa^2}{4\pi}\Lambda, \tag{3.4}$$

where $\Lambda \simeq (0.116 - \ln k\xi)$ and ξ is the vortex coherence length. The circulation associated with each vortex line is $\kappa = h/2m_n$, where m_n is the mass of a neutron and h is Planck's constant. Typically $2 \leq \Lambda \leq 10$ in the inner crust (Link & Epstein 1991). The relative importance of tension is determined by the value of the stiffness parameter $\tau = \widehat{T} r_o / F_p \bar{l}$, where F_p is the maximum pinning force, r_o is the range of the pinning potential, and $\bar{l}$ is the distance between pinning sites (Link & Epstein 1991). We take $F_p = U_o/r_o$, where U_o is the effective pinning energy per nucleus. In terms of fiducial values the stiffness τ is,

$$\tau \simeq 100 \left(\frac{\rho_s}{10^{14}\ \mathrm{g\ cm^{-3}}}\right) \left(\frac{U_o}{100\ \mathrm{keV}}\right)^{-1} \left(\frac{r_o}{10\ \mathrm{fm}}\right)^{2} \left(\frac{\bar{l}}{50\ \mathrm{fm}}\right)^{-1}. \tag{3.5}$$

The critical angular velocity difference above which the Magnus force prevents vortex pinning is $\omega_c \simeq F_p / r \rho_s \kappa \bar{l}$.

The number of pinning sites involved in an unpinning event is determined by the value of τ. When $\tau > 1$, many pinning bonds must be broken for a vortex segment to unpin. Exact expressions for the activation energy in this limit can be found in (Link & Epstein 1991). In the limiting cases of $\omega << \omega_c$ and $\omega \simeq \omega_c$, $E_a(\omega)$ is (eq. B.12 and eq. 5.1, Link & Epstein 1991),

$$E_a(\omega) \simeq \begin{cases} 2.18 U_o \sqrt{\tau} \left(\frac{\omega_c}{\omega}\right) & \omega << \omega_c \\ 5.11 U_o \sqrt{\tau} (1 - \frac{\omega}{\omega_c})^{5/4} & \omega \simeq \omega_c. \end{cases} \tag{3.6}$$

The simulations presented here use the exact expressions for E_a given in Link & Epstein (1991).

Thermal Dynamics

Changes in the local temperature affect the vortex creep rate and hence the rotation rate of the star. A temperature enhancement generates a thermal wave which propagates through the star according to the non-linear thermal diffusion equation

$$c_v \frac{\partial T}{\partial t} = \nabla \cdot (\kappa_T \nabla T) + H_{\rm friction} - \Lambda_\nu. \tag{3.7}$$

Here c_v is the specific heat and κ_T is the thermal conductivity, both of which depend on density and temperature. The internal heating rate from friction between the superfluid and crust is $H_{\rm friction}$, and Λ_ν is the cooling rate through neutrino emission. The heating rate due to superfluid friction (Chapter 2, eq. 2.7) is,

$$H_{\rm friction} = \int dI_s |\dot{\Omega}_s(\mathbf{r}, t)| \omega(\mathbf{r}, t). \tag{3.8}$$

Recall, $\omega \equiv \Omega_s - \Omega_c$ is the difference in rotation rate between the superfluid and the crust.

Relevant cooling mechanisms include neutrino cooling via the modified URCA process, neutron-neutron and neutron-proton bremsstrahlung in the core (Friman & Maxwell 1979), and electron bremsstrahlung (Itoh et al. 1984) in the crust. The neutrino cooling rates are:

$$\Lambda_\nu^{\rm URCA} = 1.8 \times 10^{21} m_n^{*3} m_p^* \left(\frac{\rho}{\rho_o}\right)^{2/3} T_9^8 \text{ ergs cm}^{-3} \text{ s}^{-1} \tag{3.9}$$

$$\Lambda_\nu^{\rm nn} = 4.4 \times 10^{19} m_n^{*4} \left(\frac{\rho}{\rho_o}\right)^{1/3} T_9^8 \text{ ergs cm}^{-3} \text{ s}^{-1} \tag{3.10}$$

$$\Lambda_\nu^{\rm np} = 5.0 \times 10^{19} m_n^{*2} m_p^{*2} \left(\frac{\rho}{\rho_o}\right)^{2/3} T_9^8 \text{ ergs cm}^{-3} \text{ s}^{-1} \tag{3.11}$$

$$\Lambda_\nu^{\rm brem} = 1.6 \times 10^{20} \left(\frac{Z^2}{A}\right) \left(\frac{\rho}{\rho_o}\right) T_9^6 \text{ ergs cm}^{-3} \text{ s}^{-1}, \tag{3.12}$$

where m_n^* is the ratio of the effective mass to the bare mass of the neutron, and similarly for the proton. We take $m_n^* = m_p^* = 0.8$ in our calculations (Bäckman, Källman & Sjöberg 1973). Our values for A (the ion mass number) and Z (the ion proton number) are from Lattimer et al. (1985), and T_9 is the internal temperature in units of 10^9 K.

We take the surface of the star to cool through blackbody radiation,

$$L_{bb} = 4\pi\sigma R_\infty T_{s,\infty}^4, \tag{3.13}$$

where R_∞ and $T_{s,\infty}$ are the radius and surface temperature seen by a distant observer. These quantities are related to their values at the surface as described in Chapter 2 (eq. 2.10).

The specific heat of the star is due predominantly to degenerate electrons (Glen & Sutherland 1980) with significant contributions from the ions at lower densities (Van Riper 1991; see Chong & Cheng 1994 for corrections). The thermal conductivity is a function of density and temperature. We use the results of Itoh et al. (1983; 1984) and Mitake, Ichimaru & Itoh (1984) for a pure crust.

Impurities may arise in the crust as a result of the cooling history of the star (Flowers & Ruderman 1977). Early in the star's thermal evolution ($T \simeq 10^{10}$ K) lattice crystallization occurs more quickly than thermal equilibration processes. Consequently, nuclei with different nuclear charge (impurities) from the dominant nuclei are likely to be formed (Flowers & Ruderman 1977; Jones 1999). The concentration of impurities lowers the mean-free-path of the electrons, reducing the thermal conductivity in the crust. The electron-impurity thermal conductivity $\kappa_{T,Q}$ is (see e.g. Ziman 1972, eq. 7.92),

$$\kappa_{T,Q} = \frac{\pi^2 n_e k^2 T}{3 m_e^*} \tau_{eQ}, \tag{3.14}$$

where n_e is the density of electrons, m_e^* is the effective mass of the electron, k is the Boltzmann constant, and τ_{eQ} is the electron-impurity relaxation time. For a high concentration of impurities, the impurity relaxation time can be approximated by the electron-ion relaxation time (Yakovlev & Urpin 1980).

$$\tau_{ei} = \frac{p_F^2 v_F}{4\pi Z^2 e^4 n_N} \Lambda_{ei}^{-1}, \tag{3.15}$$

where p_F and v_F are the momentum and velocity of an electron at the Fermi surface and $\Lambda_{ei} = \ln[(2\pi Z/3)^{1/3}(1.5 + 3/\Gamma)^{1/2}] - 1$. The ion density is n_N and Γ is the lattice

order parameter. To obtain a lower limit on the thermal conductivity for an impure crust we calculate the conductivity due to electron-ion scattering, treating the ions as if they were liquified (see discussion in Brown 2000). We obtain the liquid-state thermal conductivity numerically, using the results of Itoh et al. (1983) and Mitake et al. (1984). We also use the liquid-state neutrino emissivity (Haensel, Kaminker & Yakovlev 1996) in this case.

Models

We consider the transfer of angular momentum from the superfluid to the crust through two mechanisms: 1) a deposition of thermal energy which liberates pinned vortex lines from their pinning barriers (thermal glitch) and 2) mechanical motion of vortices (mechanical glitch). The first case would arise from the heat deposition associated with a starquake. The second case applies if crust cracking occurs by direct vortex forces as a result of strong pinning (Ruderman 1991), or through magnetic stresses arising from the forcing of the field through the crust by core vortices (Ruderman, Zhu & Chen 1998). The second case would also apply to a catastrophic unpinning event (Cheng et al. 1988; Alpar & Pines 1993; Mochizuki & Izuyama 1995). In both models, the vortices are allowed to creep as described above. We initiate vortex motion in both models at a density of 1.5×10^{14} g cm^{-3}, representative of the densest regions of the inner crust, where the contribution to the moment of inertia of pinned superfluid is largest. Since this density is near nuclear density, where the lattice is expected to dissolve, our treatment also models core-driven glitches when the

vortex motion occurs near the crust-core boundary (Ruderman, Zhu & Chen 1998).

Sudden vortex motion generates heat. For a glitch which conserves angular momentum, the heating associated with the vortex motion $E_{\rm motion}$ is determined by the change in rotational energy. Angular momentum conservation gives

$$I_c \Delta\Omega_c + \int dI_s \Delta\Omega_s = 0. \tag{3.16}$$

The heat liberated is

$$E_{\rm motion} = \Delta \left[\frac{1}{2} I_c \Omega_c^2 + \frac{1}{2} \int dI_s \Omega_s^2 \right] = \int dI_s \omega(\mathbf{r}) \Delta\Omega_s(\mathbf{r}). \tag{3.17}$$

Here $\omega(\mathbf{r})$ is the angular velocity lag before the glitch, and $\Delta\Omega_s(\mathbf{r})$ is the change in the superfluid angular velocity due to vortex motion.

If vortices unpin in a mechanical glitch, vortex drag will limit the spin-up timescale to $\sim$ 100 rotation periods (Epstein & Baym 1992) or $\sim$ 1 minute in the slowest rotating pulsar considered in our analysis. If vortex motion occurs through motion of crust material with little unpinning of vortices, the spin-up timescale is approximately the distance the vortices move divided by the transverse sound speed in the crust, $t \lesssim \Delta r / c_t \simeq 10^{-4}$ s, a small fraction of a rotation period. Since these timescales are shorter than any time-resolved glitch observations, we approximate the spin-up timescale for mechanical glitches as infinitely fast.

Geometry

A complete treatment of the thermal and rotational dynamics described above would require a multi-dimensional analysis. The energy deposition due to a starquake would likely occur in a localized region (Link, Franco & Epstein 1998; Franco, Link

& Epstein 2000); the subsequent thermal diffusion probably lacks any simple symmetry, making the vortex dynamics complicated. Moreover, the heat dissipated by a moving vortex depends on position along the line, further complicating the dynamics. These effects make the coupled thermal/rotational dynamics a difficult two or three-dimensional problem. We adopt a one-dimensional (radial) treatment as a first step in modeling thermal and rotational changes, as we now describe.

The vortices of the rotating superfluid would align themselves with the rotation axis of the solid if there were no pinning. The number of vortex lines present in the superfluid is

$$N = \frac{2\pi R^2 \Omega_s}{\kappa} \simeq \frac{10^{16}}{P}, \tag{3.18}$$

where P is the spin period in seconds. A bundle of ΔN vortex lines has ΔN times the circulation and therefore $(\Delta N)^2$ times the tension of a single line (eq. 3.4) and effectively resists bending. Consequently, a bundle of vortices tends to remain straight and aligned with the rotation axis even when forces vary along the bundle. We therefore treat the vortex array as infinitely stiff over the dimensions of the crust and average the vortex creep velocity along a vortex. In this approximation, the vortices are always aligned with the rotation axis of the crust. We take the vortex distribution to be cylindrically symmetric, and follow changes in the superfluid rotation rate as a function of the distance from the rotation axis.

We follow thermal changes in the star by solving the thermal diffusion equation (eq. 3.7) with spherical symmetry. Though a crude approximation, this treatment of the thermal evolution captures the essence of the dynamics while conserving energy.

We account for the cylindrically-symmetric vortex heat generation in the following way. The heating rate due to superfluid friction (which is always present; eq. 3.8), and the heat due to sudden vortex motion (eq. 3.17) are integrated over each cylindrical shell associated with the superfluid in the inner crust. The total heat is then divided by the volume of the spherical shell at the same radius as the cylindrical shell to find the heat deposited per unit volume, which is included as a source term in the spherical treatment of the thermal diffusion. This approach underestimates the effect of the superfluid heating terms by distributing the heat uniformly throughout the crust. We begin the stellar core at nuclear density and treat it as isothermal. The surface temperature is obtained by matching the surface temperature to the internal temperature using the prescription of Gudmundsson, Pethick & Epstein (1982) with equation 3.13 as a boundary condition on the heat flux.

Simulations

We model a $1.4M_{\odot}$ neutron star using the equation of state of Friedman & Pandharipande (1981). The stellar radius is 10.5 km and the central density is $\sim 1.3 \times 10^{15}$ g cm^{-3}. The moment of inertia of the effective crust (which includes the mass of the core plus the solid crustal lattice) is $I_c = 7.8 \times 10^{44}$ g cm^2. To compare with observed glitches, we begin our simulations using values of the spin parameters $(\Omega, \dot{\Omega})$ reported from observations. We take the temperature of the Crab pulsar to be approximately half its observed upper limit (Becker & Ashenbach 1995). We choose Vela's temperature in the middle of the observationally determined range (Seward et al. 2000).

Table 4. Physical parameters for the four pulsars used in our glitch simulations.

Pulsar	$t_{\rm age} \equiv \Omega_c/2\lvert\dot{\Omega}_c\rvert$ (yr)	Ω_c (rad s^{-1})	$\lvert\dot{\Omega}_c\rvert$ (rad s^{-2})	$T_{\rm int}$ (K)	$T_{s,\infty}$ (K)
0531+21	1.2×10^3	189	2.4×10^{-9}	8.6×10^7	7.9×10^5
0833-45	1.1×10^4	70.4	1.0×10^{-10}	7.3×10^7	7.2×10^5
1822-09	2.3×10^5	8.2	5.6×10^{-13}	7.2×10^7	7.1×10^5
0355+54	1.2×10^6	40.2	1.1×10^{-12}	6.8×10^7	6.9×10^5

For the older pulsars PSR 1822-09 and PSR 0355+54 we take temperatures consistent with standard cooling models which include superfluid effects (Van Riper 1991). Temperatures and spin parameters for the pulsars in our study are listed in Table 4.

We solve for the initial lag $\omega(\mathbf{r}, t = 0)$ numerically using equation 3.2 with the spin-down rate set equal to the observed value. As the star evolves we solve the thermal diffusion equation for the internal temperature. The vortex creep velocity is then obtained using equation 3.3. Once the creep velocity is known, equation 3.2 is solved for the superfluid rotation rate as a function of location in the star. Equation 3.1 is used to obtain the angular velocity of the crust. When the angular velocity of the superfluid and the crust are known the lag is updated as the difference between the two and the entire process is repeated. We evaluate the vortex stiffness τ at a density of 1.5×10^{14}g cm^{-3}. We chose a lattice spacing of $\bar{l}$= 50 fm which represents an average value for the inner crust (see Link & Epstein 1991; Link, Epstein & Baym 1993). We vary the pinning parameters U_0 and r_0 to obtain the best fit to the data, and take them to be constant throughout the crust. At each time step the internal temperature is updated using the thermal diffusion equation (eq. 3.7). We initiate a

thermal glitch in the neutron star with the deposition of a radial gaussian heat pulse with a full width of 40 meters at a density of 1.5×10^{14}g cm^{-3}. Density changes in the inner crust are not significant over this length scale, so the deposition is isolated to a high density region. After the thermal pulse, we solve for the thermal and rotational response of the star. A thermal glitch occurs in two phases. The initial energy deposition generates a quick response from the superfluid and the remainder of the spin change occurs as the thermal pulse propagates through the region. The angular velocity lag is reduced as a result of the glitch, which in turn decreases the coupling between the superfluid and the crust. As a result, the external torque acts on a smaller moment of inertia and the star spins down at a greater rate than before the glitch. Following the initial spin jump the superfluid relaxes and eventually the lag is recovered. In colder stars, which have a lower specific heat, the energy deposition causes a larger increase in temperature which generates a faster glitch than the same energy deposition would in a younger star.

Our results depend on the location of the energy deposition. Less energy is required when the deposition location is at lower density to produce a similar spin response, holding all other parameters constant. A wider pulse requires more total energy to generate the same spin response.

We initiate a mechanical glitch by changing the superfluid angular velocity from its steady-state value in a radial gaussian profile with a full width of 40 meters, centered at a density of 1.5×10^{14}g cm^{-3}. Sudden movement of the superfluid vortices generates heat, as described above (see eq. 3.17). After the initial angular velocity

Table 5. Internal parameters for the thermal glitch simulations.

Pulsar	U_0 (keV)	$\overline{\omega}$ (rad s^{-1})	r_0 (fm)	Δ E (ergs)	χ^2/dof	χ^2/dof (preglitch)
0531+21	18	0.08	1.2	1.5×10^{42}	10.5	11.2
0833-45	470	0.62	8.7	6.5×10^{42}	0.55	0.55
1822-09	610	1.24	5.6	4.3×10^{41}	1.2	1.0
0355+54	62	0.08	8.0	7.0×10^{42}	15.0	19.8

Table 6. Internal parameters for the mechanical glitch simulations.

Pulsar	U_0 (keV)	$\overline{\omega}$ (rad s^{-1})	r_0 (fm)	χ^2/dof	χ^2/dof (preglitch)
0531+21	18	0.09	1.1	52.3	11.2
0833-45	220	0.57	4.2	0.84	0.55
1822-09	520	1.18	4.9	0.52	1.0
0355+54	100	0.19	6.1	11.1	19.8

change, we solve for the thermal and rotational response of the star. A mechanical glitch occurs in one step as the vortex lines are moved from their steady state location. As in the thermal case, the angular velocity lag is reduced as a result of the glitch, and the star spins down at a greater rate than before the glitch. Following the initial spin jump the superfluid relaxes and eventually the lag is recovered.

A larger change in the superfluid angular velocity is required to produce the same spin response if the vortex motion occurs at lower density, holding all other parameters constant. A wider pulse requires a smaller peak value in the gaussian profile.

The thermal pulse associated with a mechanical glitch is orders of magnitude smaller than that resulting from a thermal glitch. This difference occurs because the heat deposition required to mobilize pinned vortices in a thermal glitch is larger than the heat generated by vortex motion in a mechanical glitch.

The parameters which best fit the observational data, along with the χ^2/dof, are listed in Tables 5 and 6 for the thermal and mechanical glitch models, respectively. For comparison, the χ^2/dof of the steady state observations is given (preglitch χ^2/dof) as a measure of the inherent scatter in the data. We report values for $U_o, r_o, \Delta E$ and $\bar{\omega}$, where ΔE is the energy required to produce a thermal glitch, and $\bar{\omega}$ is the angular velocity difference between the superfluid and the crust, averaged over the superfluid moment of inertia.

PSR 0531+21 (Crab Pulsar)

Simulations of the 1988 glitch in the Crab pulsar (Lyne, Smith & Pritchard 1992) are shown in Figure 6. The glitch is best modeled by a thermal glitch triggered by an energy deposition of 1.5×10^{42} ergs (solid line). The sudden change in superfluid angular momentum, initiated by the thermal pulse, is transferred to the crust giving an initial spin-up over minutes. As the thermal pulse dissipates, the remaining spin-up occurs over approximately one day. The glitch has a fractional increase in rotation rate of $\Delta\nu/\nu \simeq 7 \times 10^{-8}$. The mechanical glitch model is unable to simulate the gradual rise of the Crab observations. In this case the full spin-up occurs quickly, followed by decay of the spin increase (Fig. 6, dashed line). The thermal pulse associated with the thermal glitch peaks at the stellar surface $\sim$ 20 days after glitch

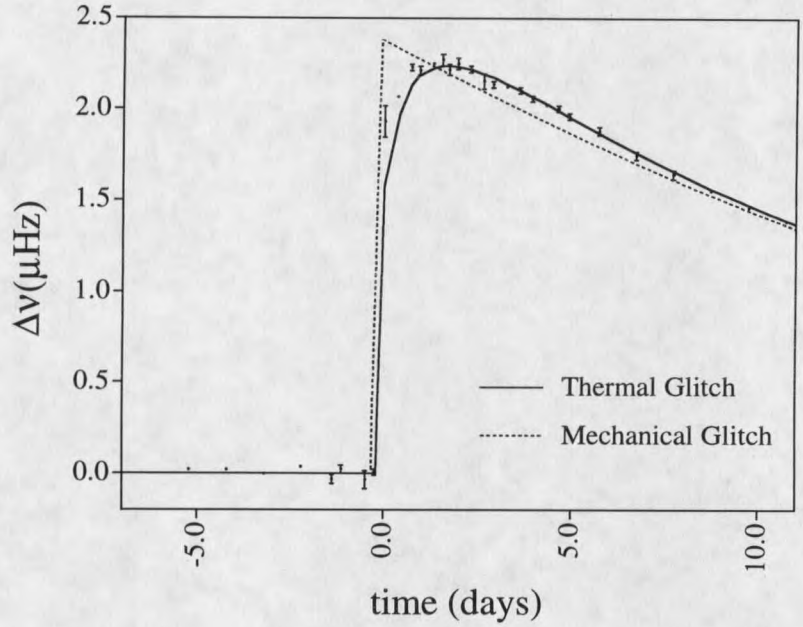

Figure 6. A thermal glitch and a mechanical glitch in the Crab pulsar. The thermal glitch occurs after an energy deposition of 1.5×10^{42} ergs. The mechanical glitch results from the sudden motion of superfluid vortex lines. Data from the 1988 glitch are shown (Lyne, Smith & Prichard 1992).

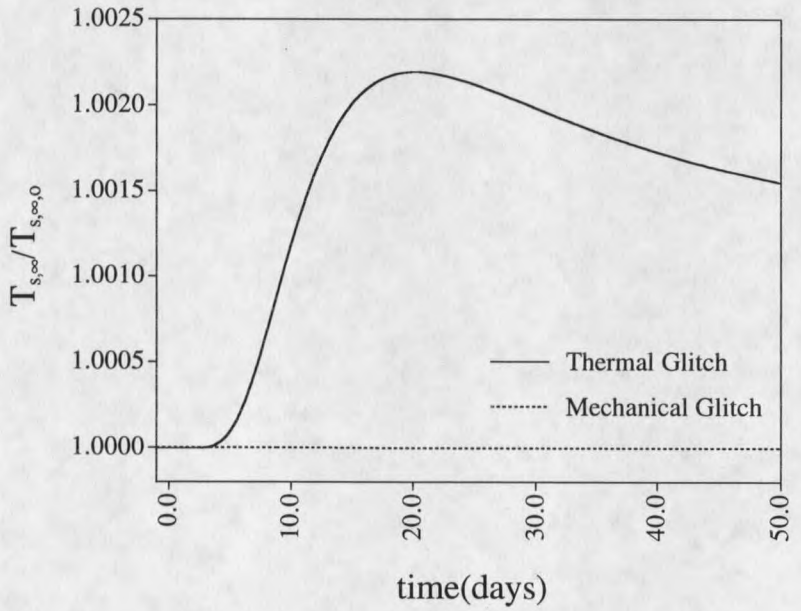

Figure 7. Surface temperature changes in the Crab pulsar after a glitch. The responses shown are following a thermal and mechanical glitch in a pure crust model.

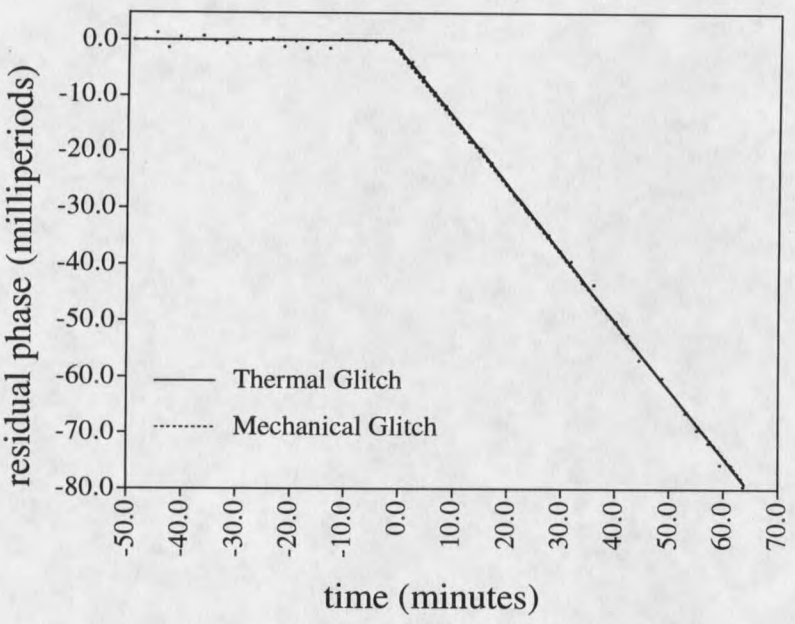

Figure 8. A thermal glitch and a mechanical glitch in the Vela pulsar. The thermal glitch is after an energy deposition of 6.5×10^{42} ergs and the mechanical glitch results from the sudden motion of superfluid vortex lines. Data from the 1989 "Christmas" glitch are shown (McCulloch et al. 1990).

onset and shows a maximum temperature increase of $\sim 0.2\%$ (Fig. 7, solid line). The surface temperature increase associated with the mechanical glitch is of negligible magnitude.

PSR 0833-45 (Vela Pulsar)

The 1989 "Christmas" glitch ($\Delta\nu/\nu \simeq 2 \times 10^{-6}$) in the Vela pulsar (McCulloch et al. 1990) is well modeled as either a thermal or mechanical glitch (Fig. 8); the simulations are virtually indistinguishable. However, the thermal pulse which reaches the stellar surface differs significantly between the two mechanisms, with a thermal

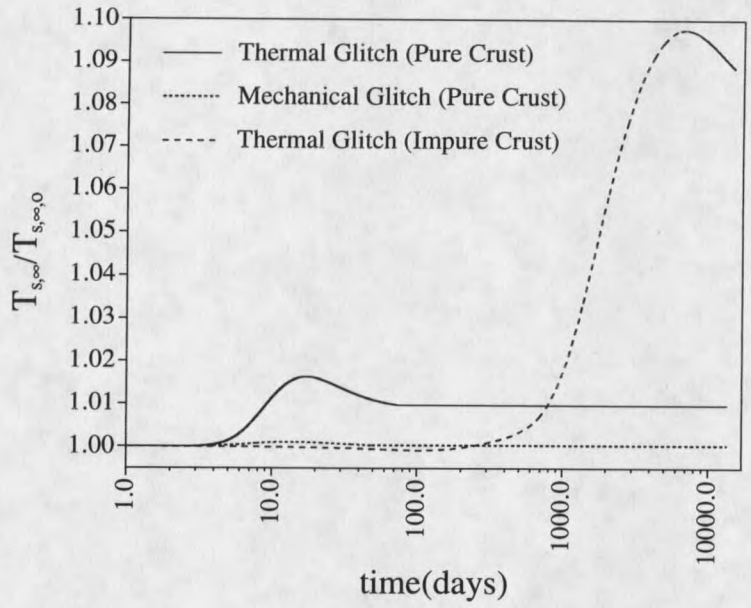

Figure 9. Surface temperature changes in the Vela pulsar after a glitch. The *dashed-dot* line shows the surface temperature response for a highly impure crust after a thermal glitch. These curves correspond to a glitch of magnitude, $\Delta\nu/\nu \simeq 3 \times 10^{-6}$, as was observed in the Vela pulsar in January 2000.

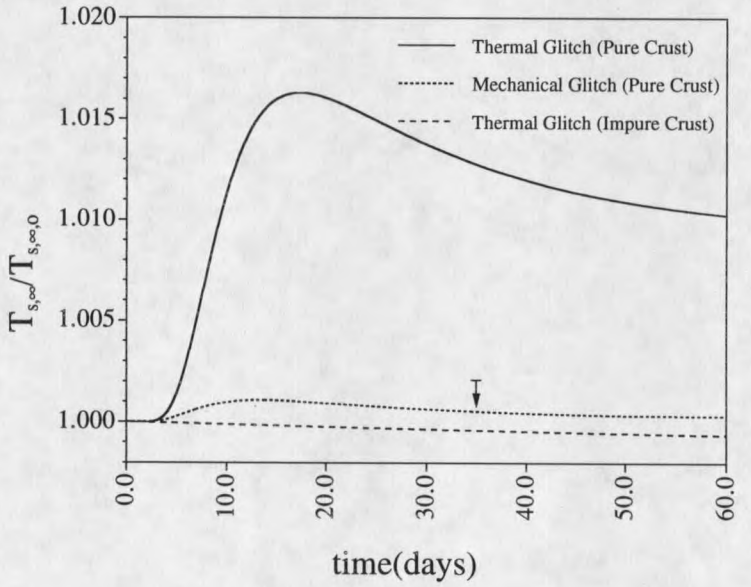

Figure 10. The first few months of the surface changes in Fig. 9. A thermal observation 35 days after the January 2000 glitch is indicated (Helfand et al. 2000; Pavlov et al. 2000).

glitch generating a pulse approximately 2 orders of magnitude larger than that resulting from the mechanical glitch (Fig. 9). Observations of thermal emission from the surface following a glitch of similar magnitude ($\Delta\nu/\nu \simeq 3.1 \times 10^{-6}$) in the Vela pulsar on January 16, 2000 limit the temperature difference to $< 0.2\%$ 35 days after glitch onset (Helfand, Gotthelf & Halpern 2000; Pavlov et al. 2000). This upper limit is marked in Figure 10 and is inconsistent with a thermal glitch in a pure crust. All the curves in Figures 9 and 10 are for a glitch of the same magnitude as the January 2000 glitch in the Vela pulsar. Lattice impurities in the stellar crust would delay the arrival of the thermal wave at the stellar surface. The low thermal conductivity of an impure crust prevents the thermal wave from entering the core, resulting in a larger increase in the surface temperature. We find that for a highly impure crust, the thermal pulse from a thermal glitch peaks at the surface $\sim$ 16 years after the glitch, having a magnitude of $\sim 10\%$ (Fig. 9). Lowering the thermal conductivity in this manner does not effect the spin-up because vortex motion occurs over a quick timescale during the initial energy deposition. The thermal pulse in an impure crust is consistent with the January 2000 Vela temperature observation (Fig. 10). The results of our highly impure crust simulations represent an upper limit on the impurity effects. A smaller impurity fraction would decrease the time at which the thermal pulse peaks at the surface.

PSR 1822-09

Shabanova (1998) observed an extremely small glitch, with a fractional change in spin rate of only 2.0×10^{-10}, in PSR 1822-09 in September of 1994. The thermal glitch

simulation in Figure 11 (solid line) turns over slowly as the thermal wave propagates through the area, consistent with the findings of Link & Epstein (1996). Although the mechanical glitch appears to the eye to be a better fit (Fig. 11, dashed line), both models are statistically consistent with the observations, having a χ^2/dof within the scatter of the data. The thermal pulse peaks at the surface of the star approximately 16 days after glitch onset for a thermal glitch (Fig. 12) and has a maximum value of only 0.075%. There is a negligible increase in the surface temperature following a mechanical glitch.

PSR 0355+54

The largest glitch observed in any pulsar occurred in PSR 0355+54 in March 1986 with a glitch magnitude of $\Delta\nu/\nu \simeq 4.4 \times 10^{-6}$ (Shemar & Lyne 1996). The glitch is well fit by either glitch model; the simulations are indistinguishable in Figure 13. A thermal glitch generates a thermal pulse at the surface which peaks $\sim$ 17 days after glitch onset with a fractional temperature increase of $\sim$ 2% (Fig. 14, solid line). A mechanical glitch generates a thermal pulse which peaks at a magnitude of $\sim$ 0.02%, about 13 days after the initial spin up (Fig. 14, dashed line).

Discussion

In this chapter we considered two different glitch scenarios involving the movement of superfluid vortex lines near nuclear density. The thermal glitch model of Link & Epstein (1996) is consistent with all glitches modeled in this study. The mechanical glitch model involving sudden vortex motion occurs much too quickly to fit glitch data

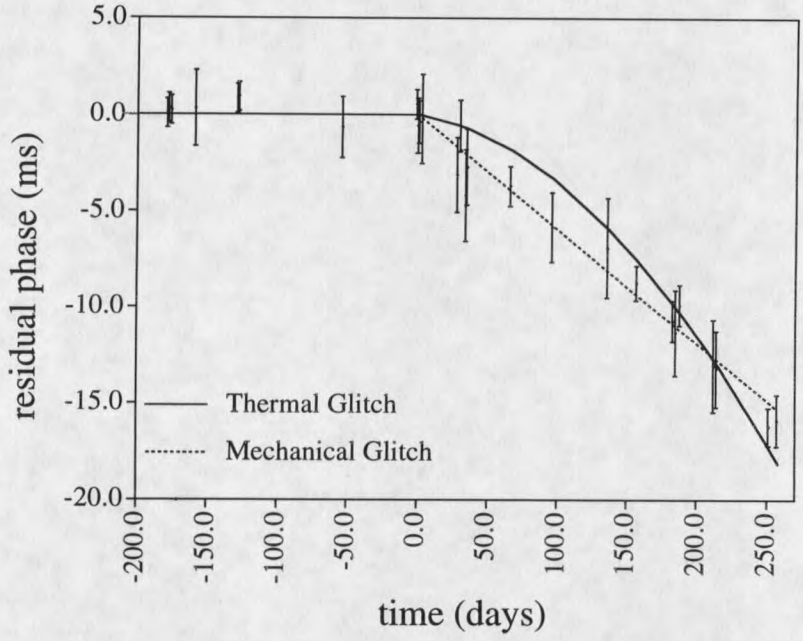

Figure 11. A thermal glitch and a mechanical glitch in PSR 1822-09. The thermal glitch occurs after an energy deposition of 4.3×10^{41} ergs. The mechanical glitch results from the sudden motion of superfluid vortex lines. Data from a 1994 glitch are shown (Shabanova 1998).

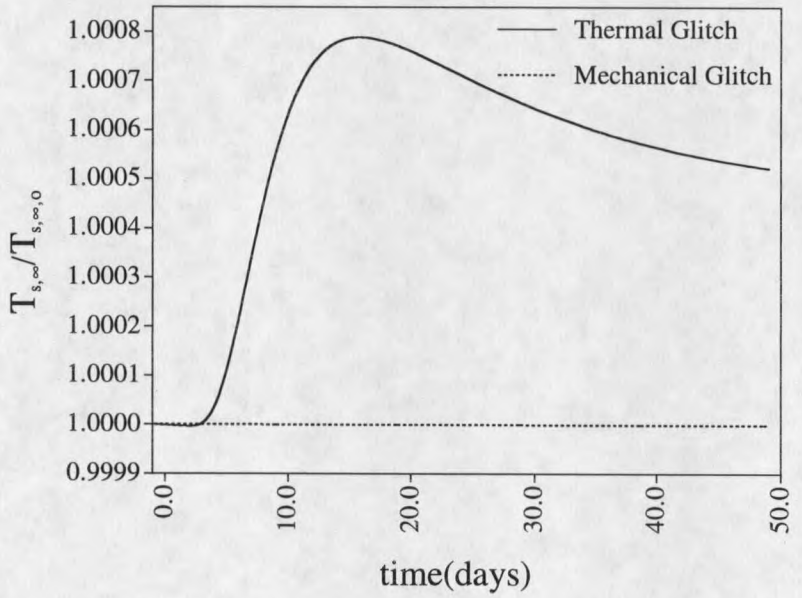

Figure 12. Surface temperature changes in PSR 1822-09 after a glitch. The responses shown are following a thermal and mechanical glitch in a pure crust model.

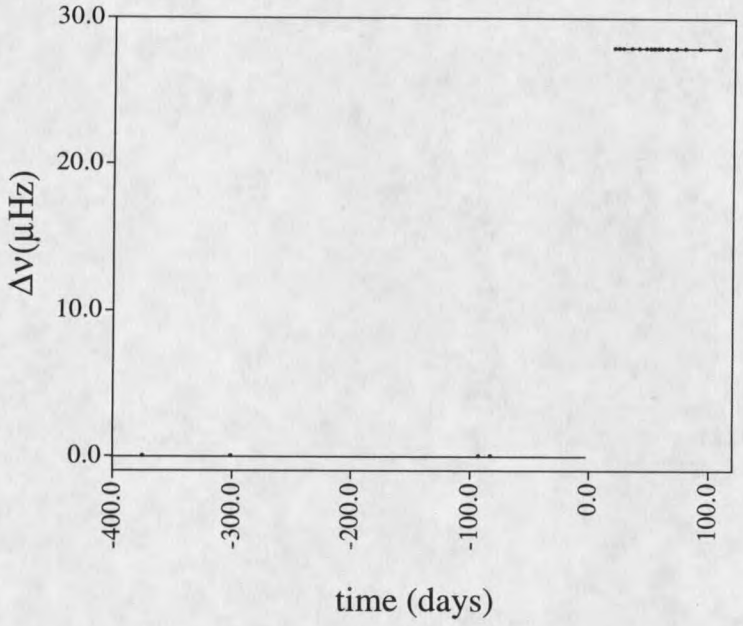

Figure 13. A thermal glitch and a mechanical glitch in PSR 0355+54. The thermal glitch occurs after an energy deposition of 7.0×10^{42} ergs. The mechanical glitch results from the sudden motion of superfluid vortex lines. The two models are indistinguishable at this scale. Data from a 1986 glitch are shown (Shemar & Lyne 1996).

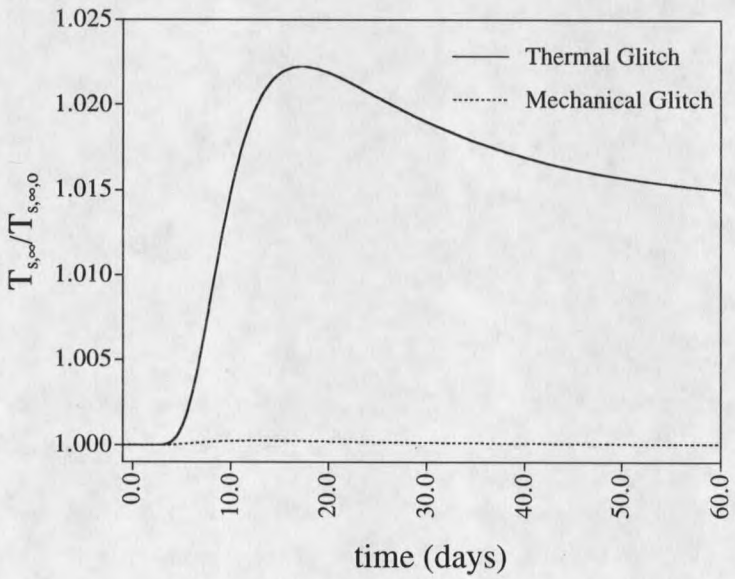

Figure 14. Surface temperature changes in PSR 0355+54 after a glitch. The responses shown are following a thermal and mechanical glitch in a pure crust model.

from 1988 in the Crab pulsar, but is consistent with glitch data in the other pulsars in our sample. However, plastic flow of the crust following a mechanical glitch, an effect we have not taken into account, might provide a slow component to the spin-up.

At present, timing measurements of glitching pulsars are too sparse to distinguish between the predicted spin behavior of thermal and mechanical glitches in most cases. However, a distinguishing feature between these models is the size of the surface temperature pulse which accompanies the glitch. The larger temperature increase associated with a thermal glitch lowers the thermal conductivity, slowing the pulse as it travels through the crust as compared to a mechanical glitch. In general, a thermal glitch exhibits a thermal pulse at the stellar surface which is much larger, and occurs a few days later, than a mechanical glitch in the same pulsar. Impurities in the stellar crust lower the thermal conductivity and could delay the surface pulse by years. A thermal glitch in an impure crust is consistent with the surface emission measurements following the January 2000 glitch in the Vela pulsar (Helfand, Gotthelf & Halpern 2000; Pavlov et al. 2000). Future glitch observations coordinated with surface emission measurements will play a key role in distinguishing between these two models by placing observational constraints on the thermal pulse which accompanies the glitch.

Time-resolved observations of slow glitch spin-up in a young pulsar (e.g., the Crab), would support the thermal glitch model. A mechanical glitch does not occur slowly enough to model such behavior, but is a viable model for glitches which spin up quickly. However, detection of an early thermal wave of large amplitude could rule

out the mechanical glitch model in a pure crust. It is also possible that both thermal and mechanical mechanisms are at work in generating pulsar glitches.

For both models we obtain effective pinning energies U_0 which range from $\sim$ 10-500 keV. These values are less than the pinning energies obtained from first-principles calculations (Pizzochero, Viverit & Broglia 1997) and may indicate the presence of tension effects which act to reduce the effective pinning energy per nucleus (Jones 1997; 1998; 1999). The lower values of U_0 we find for the Crab pulsar could indicate that glitches originate in a different pinning region for this object than in other pulsars. The values we obtain for the range of the pinning potential r_o are consistent with existing estimates (Pizzochero, Viverit & Broglia 1997; Epstein & Baym 1988). In Chapter 2 we obtained constraints on $\bar{\omega}$ in older pulsars by showing that frictional heat generated between the superfluid and the crust could account for their high observed temperatures. That work also provided upper limits on $\bar{\omega}$ in younger pulsars, by requiring that young stars be stable against a thermal-rotational instability. For stars of the same age, the values of $\bar{\omega}$ obtained from glitch simulations are in agreement with those results.

CHAPTER 4

SUMMARY

This thesis has examined several observational consequences of superfluidity on the thermal evolution and rotational dynamics of neutron stars. We considered the coupled thermal and rotational evolution of neutron stars in two regimes. Chapter 2 examined the long-term thermal evolution of neutron stars. Chapter 3 studied the short-term response of a star to perturbations in the star's temperature and rotation.

Late-time Thermal Evolution

In Chapter 2 we investigated a promising internal heat source to account for the observed temperatures of two older pulsars. This heat source is friction between the neutron star crust and the superfluid it contains. Interpreting the observed temperatures as due to frictional heat provides limits on the strength of the frictional coupling between the the superfluid and the crust. We also investigated the stability of young neutron stars against a thermal-rotational instability. By requiring that young stars be stable, we obtained upper limits on the frictional coupling parameter in those neutron stars. Our results are consistent with first-principles calculations of this coupling parameter.

Simulations of Glitches

In Chapter 3 we presented numerical simulations of pulsar glitches in order to

distinguish between two different glitch scenarios which involve movement of vortex lines near nuclear density. We obtained good fits to glitch observations in the four pulsars we studied. In addition to modeling the spin change associated with the glitch, we provided predictions for the glitch-associated thermal pulse, which could be visible from the stellar surface months to years after the glitch occurs. We found that impurities in the crust would delay the arrival of the thermal pulse at the stellar surface by up to decades. Future surface emission measurements coordinated with radio observations will constrain the physical processes responsible for glitches and the properties of the crust.

REFERENCES CITED

Abney, M., Epstein, R.I., Olinto, A., 1996, ApJ, 466, L91.

Ainsworth, T., Pines, D., Wambach, J., 1989, Phys. Lett. B, 222, 173.

Alpar, M.A., 1977, ApJ, 213, 527.

Alpar, M.A., Anderson, P.W., Pines, D., Shaham, J., 1984, ApJ, 276, 325.

Alpar, M.A., Brinkmann, W., Kızıloğlu,, Ü., Ögelman, H., Pines, D., 1987, A&A, 177, 101.

Alpar, M.A., Cheng, K.S., Pines, D., 1989, ApJ, 346, 823.

Alpar, M.A., Langer, S. A., Sauls, J. A., 1984, ApJ, 282, 533.

Alpar, M.A., Nandkumar, R., Pines, D., ApJ, 1986, 311, 197.

Anderson, P.W., Itoh, N., 1975, Nature, 256, 25.

Baade, W., Zwicky, F., 1934, Proc. Natl. Acad. Sci. USA, 20, 254.

Bäckman S.-O., Källman C.G. Sjöberg O., 1973, Phys. Letters, 43B, 263.

Baykal, A., 1997, A&A, 319, 515.

Baykal, A., Alpar, M. A., Kızıloğlu, Ü., 1991, A&A, 252, 664.

Baym, G., Chandler, E., 1983, J. Low Temp. Phys, 50, 57.

Baym, G., Pethick, C. J., Sutherland, P., 1971, ApJ, 170, 299.

Baym, G., Pines, D., 1971, Ann. Phys., 66, 816.

Becker, W., Ashenbach, B., 1995, in Lives of the Neutron Stars, ed M.A. Alpar, Ü. Kızıloğlu, J. van Paradijs (Dordrecht:Kluwer), 47.

Boynton, P. E., 1981, in *IAU Symposium 95, Pulsars*, ed. R. Wielebinski, W. Sieber, (Dordrecht: Reidel), p. 279.

Boynton, P. E., Deeter, J. E., Lamb, F. K., Zylstra G., Pravdo, S. H., White, N. E., Wood. K. S., Yentis, D. J., 1984, ApJ, 283, L53.

Carter, B., Langlois, D., Sedrakian, D.M., 2000, A&A, 361, 795.

Chau, H.F., Cheng, K.S., 1993a, in Isolated Pulsars, ed. K.A. Van Riper, R.I. Epstein, C. Ho (Cambridge Univ. Press), 35.

Chau, H. F., Cheng, K. S., 1993b, Phys. Rev. B, 47, 2707.

Chau, H.F., Cheng, K.S., Ding, X.X., 1992, ApJ, 399, 213.

Chau, H. F., McCulloch, P. M., Nandkumar, R., Pines, D., 1993, ApJ, 413, L113.

Cheng, K. S., Chau, W. Y., Zhang, J. L., Chau, H. F., 1992, ApJ, 396, 135.

Chong, N, Cheng, K.S., 1994, ApJ, 425, 210.

Cordes, J. M., Downs, G. S., Krause-Polstorff, J., 1988, ApJ, 330, 847.

Deeter, J. E., 1981, PhD thesis, University of Washington.

Dodson, R.G., McCulloch, P.M., Costa, M.E., 2000, IAUC 7347.

Downs, G.S., 1981, ApJS, 249, 687.

Eikenberry, S.S., Fazio, G.G., Ransom, S.M., 1998, ApJ, 492, 754.

Epstein, R.I., Baym, G., 1988, ApJ, 328, 680.

Epstein, R.I., Baym, G., 1992, ApJ 387,276.

Ergma, E., van den Heuvel, E.P.J., 1998, A&A, 331, L29.

Fetter, A.L., 1967, Phys. Rev., 162, 143.

Finley, J. P., Ögelman, H., Kızıloğlu, Ü., 1992, ApJ, 394, L21.

Flowers, E.G., Ruderman, M.A., 1977, ApJ, 215, 302.

Franco, L.M., Link B., Epstein R.I., 2000, ApJ, 543, 987.

Friedman, B., Pandharipande, V. R., 1981, Nucl. Phys. A, 361, 502.

Friman, B.L., Maxwell, O.V., 1979, ApJ, 232, 541.

Glen, G., Sutherland, P., 1980, ApJ, 239, 671.

Gold, T., 1968, Nature, 218, 731.

Goldreich, P., Reisenegger, A. 1992, ApJ 395, 250.

Greenstein, G., 1975, ApJ, 200, 281.

Greenstein, G., 1979a, 231, 880.

Greenstein, G., 1979b, Nature, 277 ,521.

Gudmundsson, E., Pethick, C., Epstein, R. I., 1982, ApJ, 259, L19.

Haensel, P., Kaminker, A.D., Yakovlev, D.G., 1996, A&A, 314, 328.

Hailey, C.J., Craig, W.W., 1995, ApJ, 455, L151.

Halpern, J. P., Ruderman, M., 1993, ApJ, 415, 286.

Harding, D., Guyer, R. A., Greenstein, G., 1978, ApJ, 222, 991.

Helfand, D.J., Gotthelf, E.V., Halpern, J.P., 2000, astro-ph 0007310.

Hewish, A., Bell, S.J., Pilkington, J.D.H., Scott, P.F., Collins, R.A., 1968, Nature, 217, 709.

Heyl, J.S., Kulkarni, S.R., 1998, ApJ, 506, L61.

Itoh N, Mitake S., Iyetomi H., Ichimaru S., 1983, ApJ, 273, 774.

Itoh, N, Kohyama, Y., Matsumoto, N., Seki, M., 1984, ApJ, 285, 758.

Jones, P.B., 1997, Phys. Rev. Lett., 79, 792.

Jones, P.B., 1998, MNRAS, 296, 217.

Jones, P.B., 1999, MNRAS, 306,327.

Joss, P.C. Rappaport, S.A., 1984, Ann. Rev. Astr. & Astoph., 22, 537.

Kouveliotou, C., Dieters, S., Strohmayer, T., van Paradijs, J., Fishman, G.J., Meegan, C.A., Hurley, K., Kommers, J., Smith, I., Frail, D., Murakami T., 1998, Nature, 393, 235.

Larson, M.B., Link, B., 1999, ApJ, 521, 271.

Lattimer, J.M., Pethick, C.J., Ravenhall, D.G., Lamb, D.Q., 1985, Nucl. Phys. A, 432, 646.

Link, B., Epstein, R.I., 1991, ApJ, 373, 592.

Link, B., Epstein, R.I., 1996, ApJ, 457, 844.

Link, B., Epstein, R. I., Baym, G., 1993, ApJ, 403, 285.

Link, B., Epstein, R.I. , Lattimer, J.M., 1999, PRL, 83, 17.

Link, B., Franco, L.M., Epstein, R.I., 1998, ApJ, 508, 838.

Lorenz, C.P., Ravenhall, D.G., Pethick, C.J., 1993, Phys. Rev. Lett., 70, 379.

Lyne, A.G., Smith, F.G., Pritchard, R.S., 1992, Nat, 359, 706.

Lyne, A.G., Pritchard, R.S., Graham-Smith, F., 1993, MNRAS, 265, 1003.

Lyne, A.G., Pritchard, R.S., Graham-Smith, F., Camilo, F., 1996, Nature, 381, 497.

Manchester, R.N., Newton, L.M., Durdin, J.M., 1985, Nature, 313, 374.

Manning, R.A., Willmore, A.P., 1994, MNRAS, 266, 635.

McCulloch, P.M., Hamilton, P.A., McConnell, D., King, E.A., 1990, Nat, 346, 822.

Migdal, A.B., 1959, Nucl. Phys., 13, 655.

Miller, M.C., 1992, MNRAS, 255,129.

Mitake, S., Ichimaru, S., Itoh, N., 1984, ApJ, 277, 375.

Ögelman, H., Finley, J.P., 1993, ApJ, 413, L31.

Ögelman, H., Finley, J.P., Zimmermann, H.U., 1993, Nature, 361, 136.

Pandharipande, V. R., Smith, R. A., 1975, Nucl. Phys. A, 237, 507.

Pacini, F., 1967, Nature, 216, 567.

Prakash, M., 1994, Phys. Rep. 242, 297.

Pavlov, G.G., Sanwal, D., Garmire, G.P., Zavlin, V.E., Burwitz, V., Dodson, R., 2000, AAS Mtg. 196, 37.04.

Pavlov, G.G., Stringfellow, G.S., Córdova, F.A., 1996, ApJ, 467, 370.

Pethick, C.J., Ravenhall, D.G., Lorenz, C.P., 1995, Nucl. Phys. A, 584, 675.

Pines, D., Alpar, M.A., 1985, Nat, 316, 27.

Pines, D., Shaham, J., Alpar, M.A., Anderson, P.W., 1980, Prog. Theor. Phys. Suppl., 69, 376.

Pizzochero, P. M., Viverit, L., Broglia, R. A., 1997, Phys. Rev. Lett., 79, 3347.

Reisenegger, A., 1995, ApJ, 442, 749.

Rhoades, C.E., Ruffini, R., 1974, Phys. Rev. Lett. 32, 324.

Romani, R.W., 1987, ApJ, 313, 718.

Ruderman, M., 1969, Nat, 223, 597.

Ruderman, M., 1976, ApJ, 203, 213.

Ruderman, M., 1991, ApJ, 366, 261.

Ruderman, M., Zhu, T., Chen, K., 1998, ApJ, 492, 267.

Sedrakian, A. O., Sedrakian, D. M., 1995, ApJ, 447, 305.

Sedrakian A., Cordes J.M., 1999, MNRAS, 307, 365.

Seward, F.D., Alpar, M.A., Flanagan, C., Kızıloğlu, Ü., Markwardt, C., McCulloch, P., Ögelman, H., 2000, ApJ, 536, 948.

Shabanova, T.V., 1998, A&A, 337, 723.

Shemar, S.L., Lyne, A.G., 1996, MNRAS, 282, 677.

Shibazaki, N., Lamb, F. K., 1989, ApJ, 346, 808.

Shibazaki, N., Mochizuki, Y., 1994, ApJ, 438, 288.

Smolukowski, R., 1970, Phys. Rev. Lett., 24, 923.

Thompson, C., Duncan, R.C., 1996, ApJ, 473, 322.

Thorsett S.E., Chakrabarty D., 1999, ApJ, 512, 288.

Tsuruta, S., 1998, Phys. Rep., 291, 1.

Umeda, H., Shibazaki, N., Nomoto, K., Tsuruta, S., 1993, ApJ, 408, 186.

Van Riper, K. A., 1991, ApJS, 75, 449.

Van Riper, K. A., Epstein, R. I., Miller, G. S., 1991, ApJ, 381, L47.

Van Riper, K. A., Link, B., Epstein, R.I., 1995, ApJ, 448, 294.

Walter, F.M., 2001, ApJ, 549, 433.

Wambach, J., Ainsworth, T.L., Pines, D., 1991, in Neutron Stars: Theory and Observations, ed. J. Ventura & D. Pines (Dordrecht:Kluwer), 37.

Yakovlev D.G., Urpin V.A., 1980, Soviet Astron., 24, 303.

Yancopoulos, S., Hamilton, T.T., Helfand, D., 1994, ApJ, 429, 832.

Ziman, J.M., 1972, Principles of the Theory of Solids, 2nd ed., Cambridge: Cambridge Univ. Press.